Amplitude analyses
Part II

Anton Poluektov

The University of Warwick, UK

13 September 2018

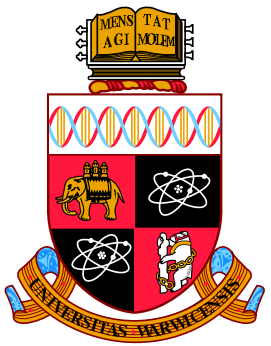

[[PRL 112 (2014) 011801]]

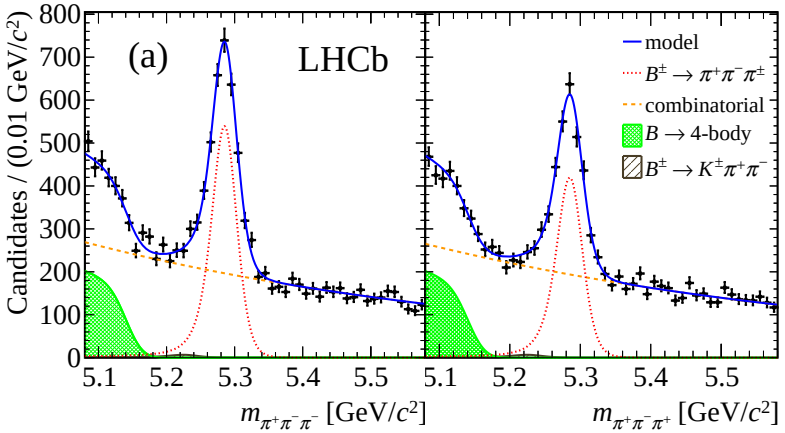

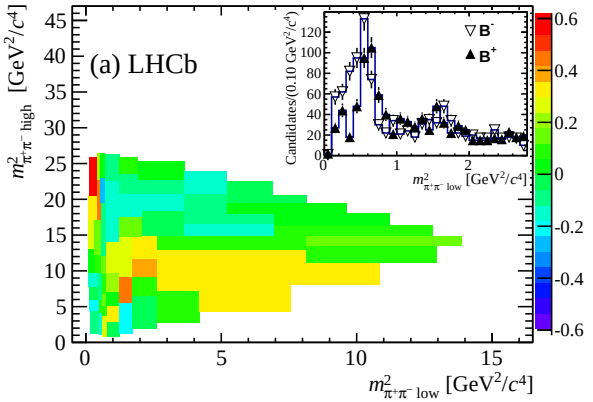

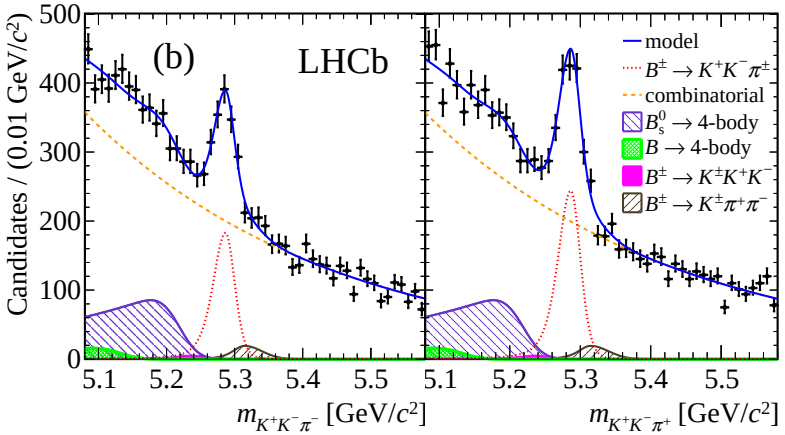

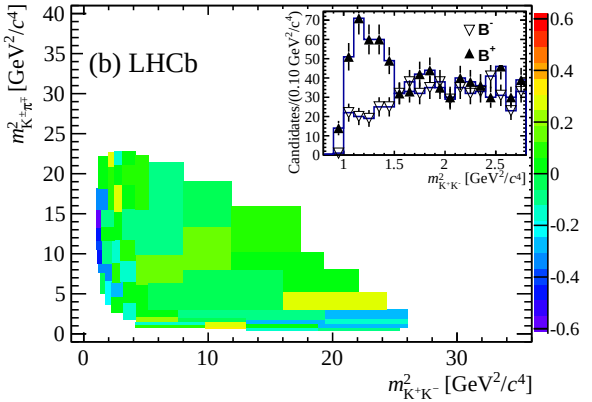

Integrated asymmetries:

$$A_{CP}(B^\pm \to \pi^\pm\pi^+\pi^-) = +0.117 \pm 0.021 \pm 0.009 \pm 0.007(J/\psi K^+)$$

$$A_{CP}(B^\pm \to \pi^\pm K^+K^-) = -0.141 \pm 0.040 \pm 0.018 \pm 0.007(J/\psi K^+)$$

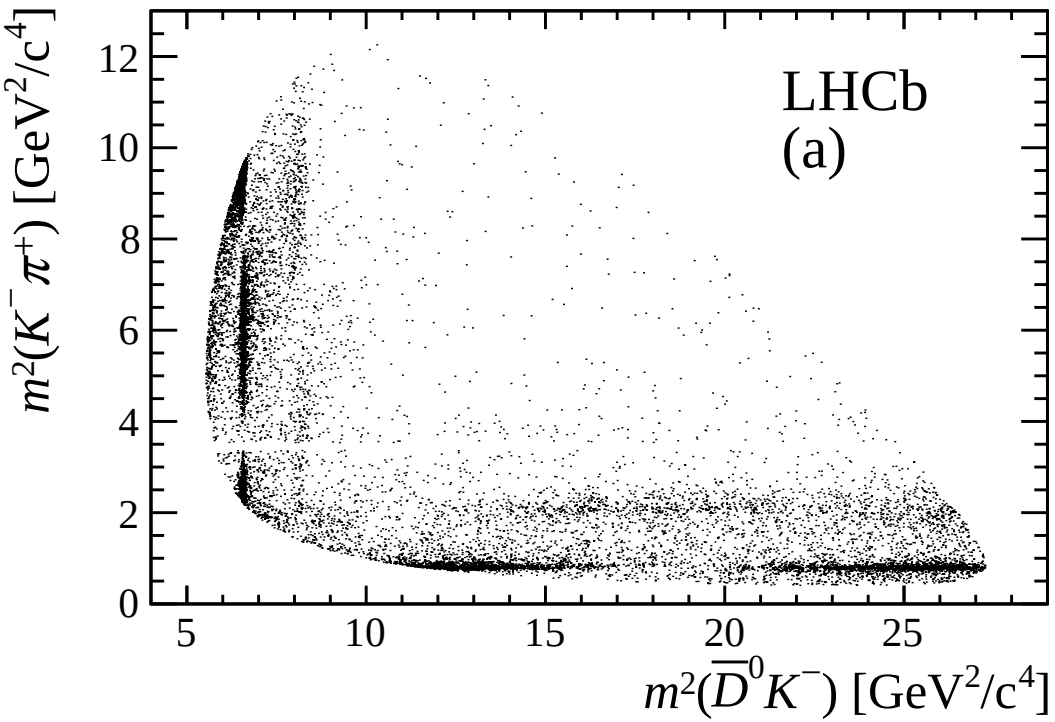

Resonance	Spin	Dalitz plot axis	Model	Parameters (MeV/c^2)
$\overline{K}^*(892)^0$	1	$m^2(K^-\pi^+)$	RBW	$m_0 = 895.81 \pm 0.19$, $\Gamma_0 = 47.4 \pm 0.6$
$\overline{K}^*(1410)^0$	1	$m^2(K^-\pi^+)$	RBW	$m_0 = 1414 \pm 15$, $\Gamma_0 = 232 \pm 21$
$\overline{K}_0^*(1430)^0$	0	$m^2(K^-\pi^+)$	LASS	See text
$\overline{K}_2^*(1430)^0$	2	$m^2(K^-\pi^+)$	RBW	$m_0 = 1432.4 \pm 1.3$, $\Gamma_0 = 109 \pm 5$
$\overline{K}^*(1680)^0$	1	$m^2(K^-\pi^+)$	RBW	$m_0 = 1717 \pm 27$, $\Gamma_0 = 322 \pm 110$
$\overline{K}_0^*(1950)^0$	0	$m^2(K^-\pi^+)$	RBW	$m_0 = 1945 \pm 22$, $\Gamma_0 = 201 \pm 90$
$D_{s2}^*(2573)^-$	2	$m^2(\overline{D}^0 K^-)$	RBW	See text
$D_{s1}^*(2700)^-$	1	$m^2(\overline{D}^0 K^-)$	RBW	$m_0 = 2709 \pm 4$, $\Gamma_0 = 117 \pm 13$
$D_{sJ}^*(2860)^-$	1	$m^2(\overline{D}^0 K^-)$	RBW	See text
$D_{sJ}^*(2860)^-$	3	$m^2(\overline{D}^0 K^-)$	RBW	See text
Nonresonant		$m^2(\overline{D}^0 K^-)$	EFF	See text
D_{sv}^{*-}	1	$m^2(\overline{D}^0 K^-)$	RBW	$m_0 = 2112.3 \pm 0.5$, $\Gamma_0 = 1.9$
$D_{s0\,v}^*(2317)^-$	0	$m^2(\overline{D}^0 K^-)$	RBW	$m_0 = 2317.8 \pm 0.6$, $\Gamma_0 = 3.8$
B_v^{*+}	1	$m^2(\overline{D}^0 \pi^+)$	RBW	$m_0 = 5325.2 \pm 0.4$, $\Gamma_0 = 0$

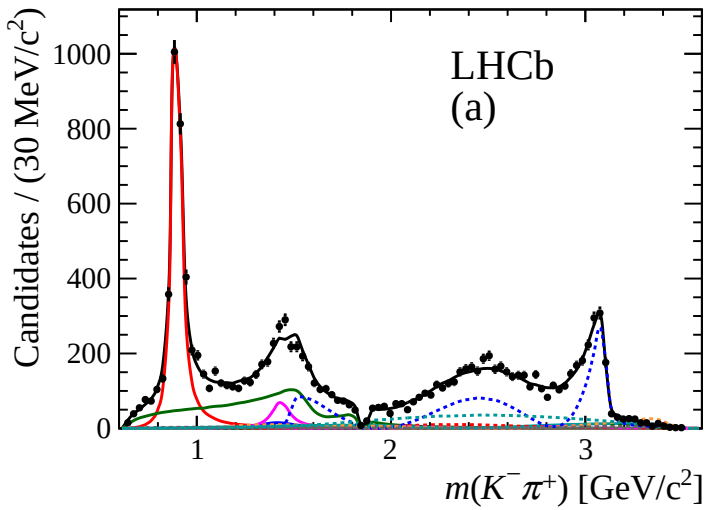

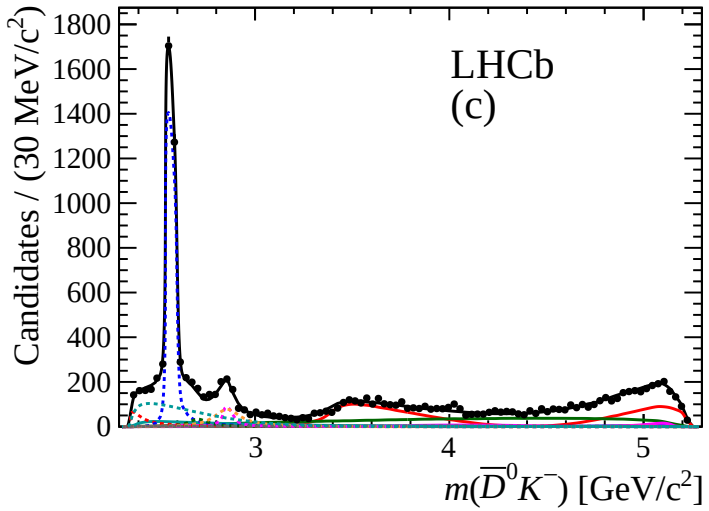

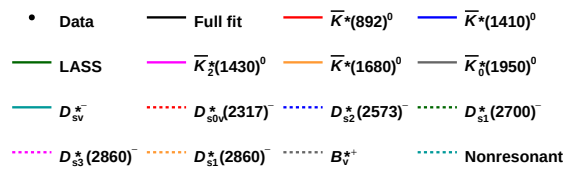

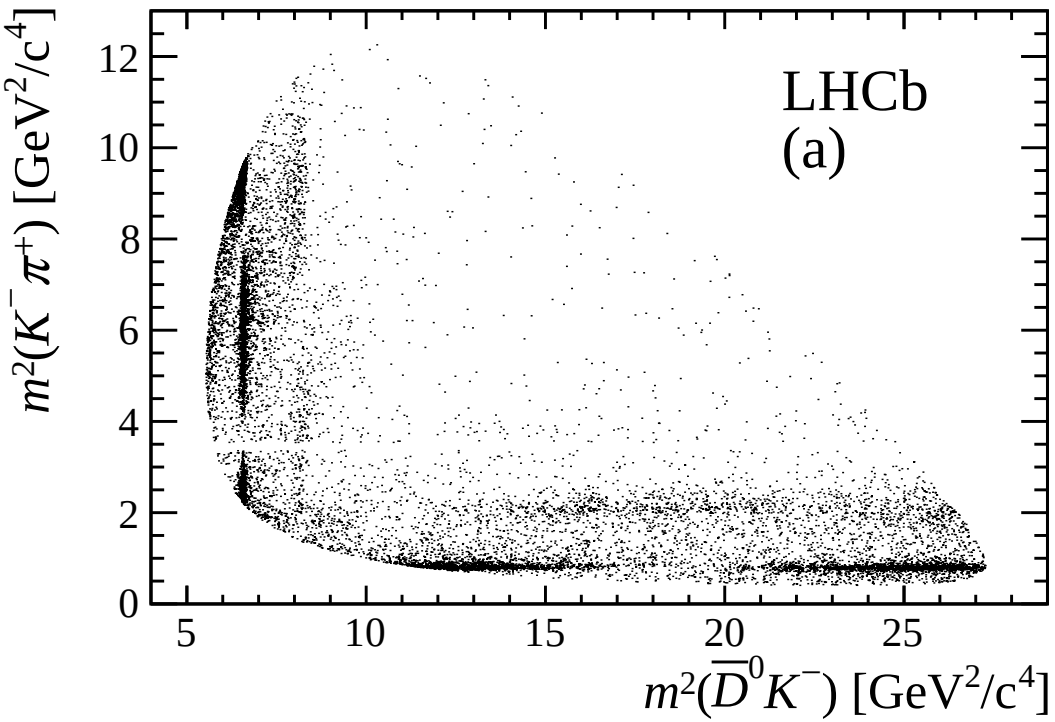

Resonance	Spin	Dalitz plot axis	Model	Parameters (MeV/c^2)
$\overline{K}^*(892)^0$	1	$m^2(K^-\pi^+)$	RBW	$m_0 = 895.81 \pm 0.19$, $\Gamma_0 = 47.4 \pm 0.6$
$\overline{K}^*(1410)^0$	1	$m^2(K^-\pi^+)$	RBW	$m_0 = 1414 \pm 15$, $\Gamma_0 = 232 \pm 21$
$\overline{K}_0^*(1430)^0$	0	$m^2(K^-\pi^+)$	LASS	See text
$\overline{K}_2^*(1430)^0$	2	$m^2(K^-\pi^+)$	RBW	$m_0 = 1432.4 \pm 1.3$, $\Gamma_0 = 109 \pm 5$
$\overline{K}^*(1680)^0$	1	$m^2(K^-\pi^+)$	RBW	$m_0 = 1717 \pm 27$, $\Gamma_0 = 322 \pm 110$
$\overline{K}_0^*(1950)^0$	0	$m^2(K^-\pi^+)$	RBW	$m_0 = 1945 \pm 22$, $\Gamma_0 = 201 \pm 90$
$D_{s2}^*(2573)^-$	2	$m^2(\overline{D}^0 K^-)$	RBW	See text
$D_{s1}^*(2700)^-$	1	$m^2(\overline{D}^0 K^-)$	RBW	$m_0 = 2709 \pm 4$, $\Gamma_0 = 117 \pm 13$
$D_{sJ}^*(2860)^-$	1	$m^2(\overline{D}^0 K^-)$	RBW	See text
$D_{sJ}^*(2860)^-$	3	$m^2(\overline{D}^0 K^-)$	RBW	See text
Nonresonant		$m^2(\overline{D}^0 K^-)$	EFF	See text
D_{sv}^{*-}	1	$m^2(\overline{D}^0 K^-)$	RBW	$m_0 = 2112.3 \pm 0.5$, $\Gamma_0 = 1.9$
$D_{s0v}^*(2317)^-$	0	$m^2(\overline{D}^0 K^-)$	RBW	$m_0 = 2317.8 \pm 0.6$, $\Gamma_0 = 3.8$
B_v^{*+}	1	$m^2(\overline{D}^0 \pi^+)$	RBW	$m_0 = 5325.2 \pm 0.4$, $\Gamma_0 = 0$

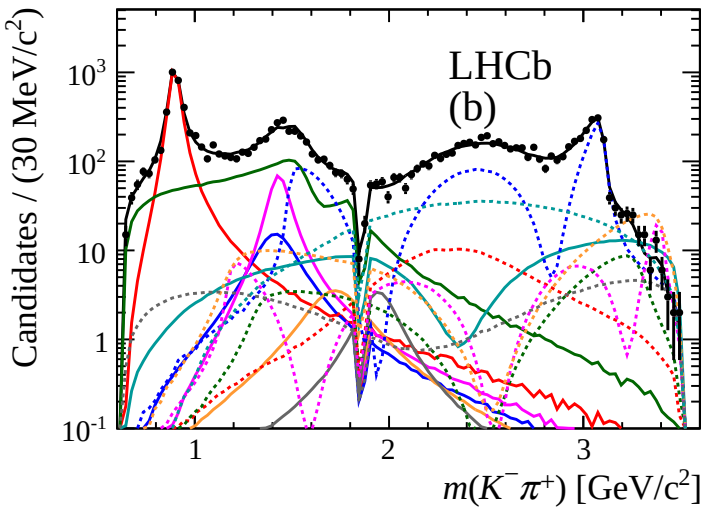

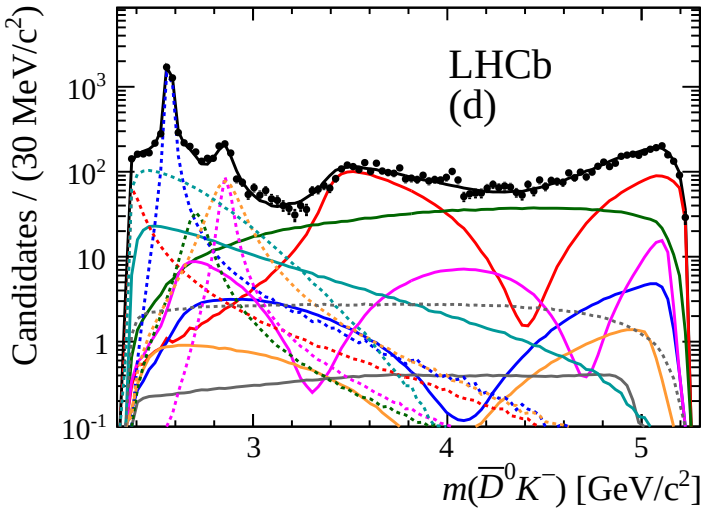

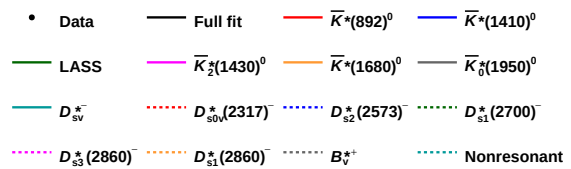

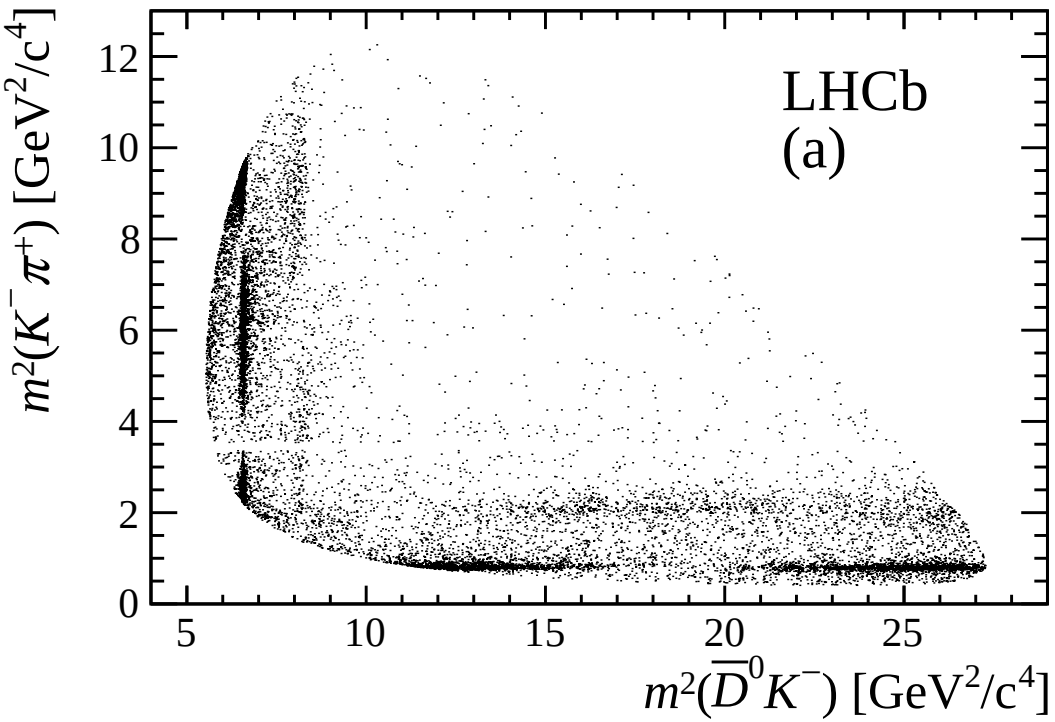

Resonance	Spin	Dalitz plot axis	Model	Parameters (MeV/c^2)
$\overline{K}^*(892)^0$	1	$m^2(K^-\pi^+)$	RBW	$m_0 = 895.81 \pm 0.19$, $\Gamma_0 = 47.4 \pm 0.6$
$\overline{K}^*(1410)^0$	1	$m^2(K^-\pi^+)$	RBW	$m_0 = 1414 \pm 15$, $\Gamma_0 = 232 \pm 21$
$\overline{K}_0^*(1430)^0$	0	$m^2(K^-\pi^+)$	LASS	See text
$\overline{K}_2^*(1430)^0$	2	$m^2(K^-\pi^+)$	RBW	$m_0 = 1432.4 \pm 1.3$, $\Gamma_0 = 109 \pm 5$
$\overline{K}^*(1680)^0$	1	$m^2(K^-\pi^+)$	RBW	$m_0 = 1717 \pm 27$, $\Gamma_0 = 322 \pm 110$
$\overline{K}_0^*(1950)^0$	0	$m^2(K^-\pi^+)$	RBW	$m_0 = 1945 \pm 22$, $\Gamma_0 = 201 \pm 90$
$D_{s2}^*(2573)^-$	2	$m^2(\overline{D}^0 K^-)$	RBW	See text
$D_{s1}^*(2700)^-$	1	$m^2(\overline{D}^0 K^-)$	RBW	$m_0 = 2709 \pm 4$, $\Gamma_0 = 117 \pm 13$
$D_{sJ}^*(2860)^-$	1	$m^2(\overline{D}^0 K^-)$	RBW	See text
$D_{sJ}^*(2860)^-$	3	$m^2(\overline{D}^0 K^-)$	RBW	See text
Nonresonant		$m^2(\overline{D}^0 K^-)$	EFF	See text
D_{sv}^{*-}	1	$m^2(\overline{D}^0 K^-)$	RBW	$m_0 = 2112.3 \pm 0.5$, $\Gamma_0 = 1.9$
$D_{s0\,v}^*(2317)^-$	0	$m^2(\overline{D}^0 K^-)$	RBW	$m_0 = 2317.8 \pm 0.6$, $\Gamma_0 = 3.8$
B_v^{*+}	1	$m^2(\overline{D}^0 \pi^+)$	RBW	$m_0 = 5325.2 \pm 0.4$, $\Gamma_0 = 0$

$D_{s2}(2573)$:

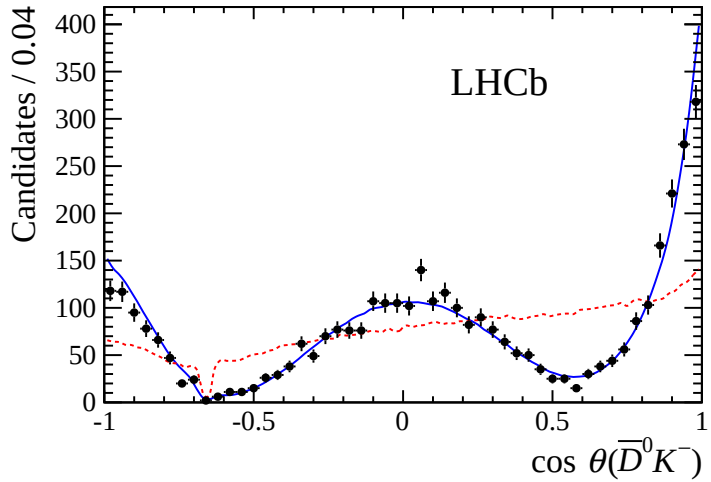

$D_{sJ}(2860)$:

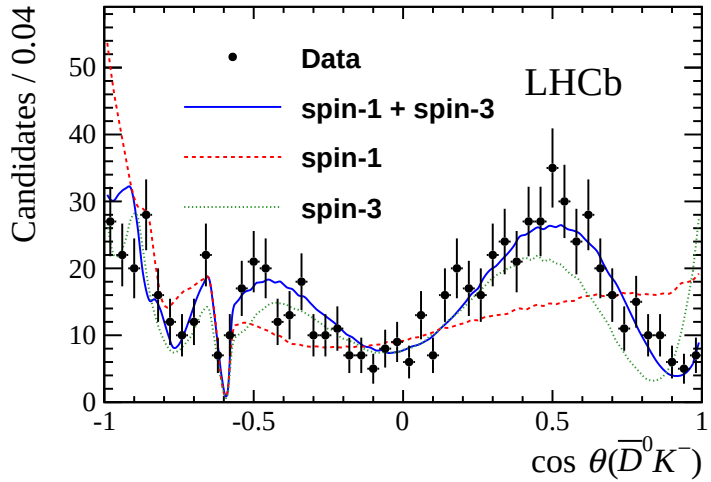

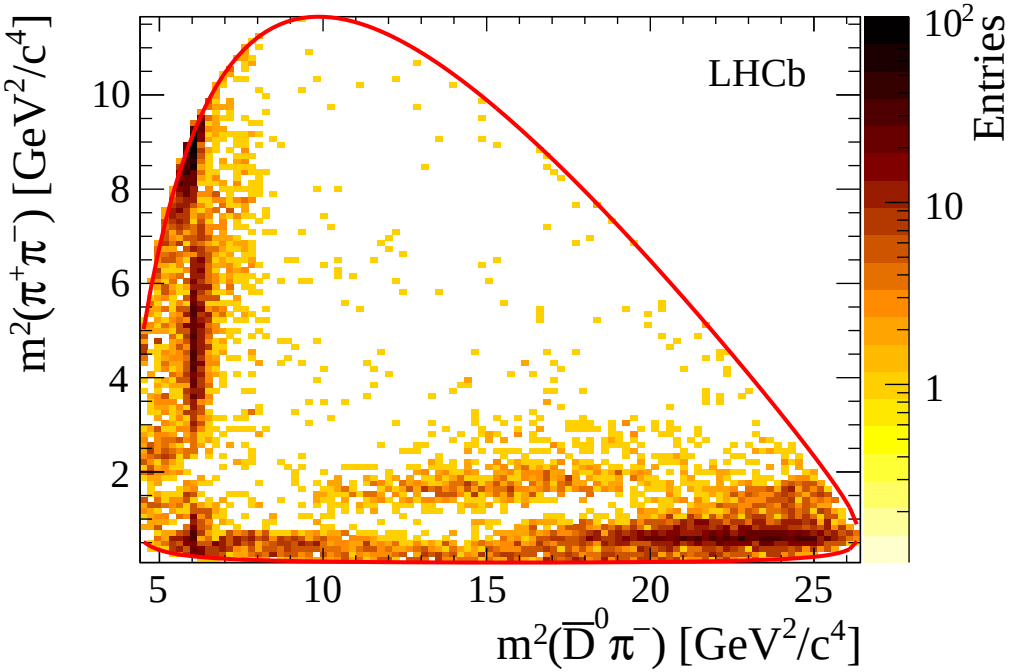

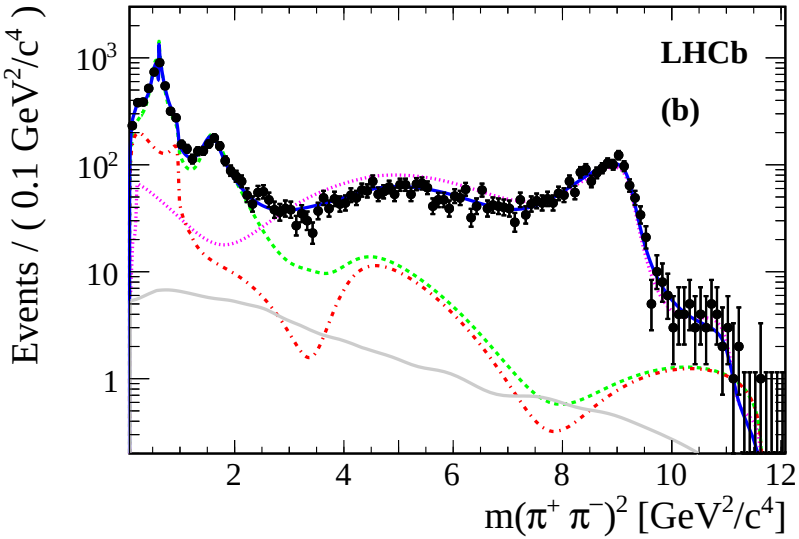

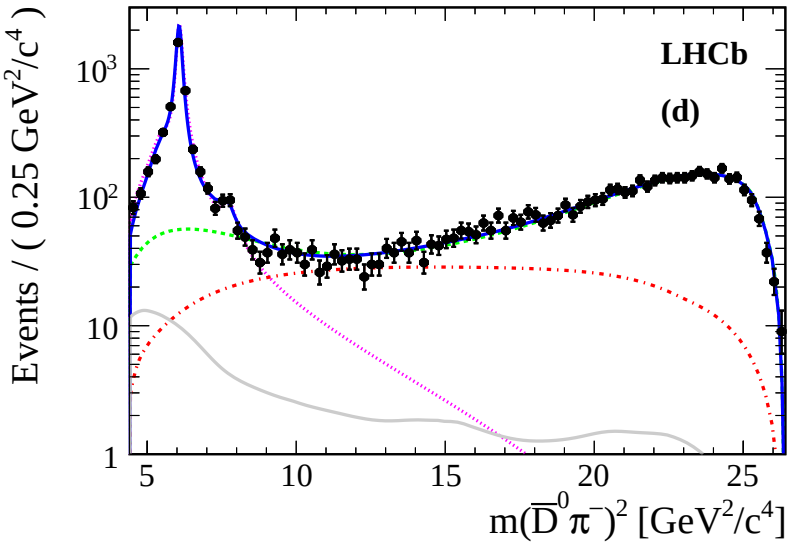

Resonance	Spin	Model	m_r (MeV/c^2)	Γ_0 (MeV)
$\bar{D}^0\pi^-$ P-wave	1	Eq. ??	Floated	
$D_0^*(2400)^-$	0	RBW	Floated	
$D_2^*(2460)^-$	2	RBW	Floated	
$D_J^*(2760)^-$	3	RBW	Floated	
$\rho(770)$	1	GS	775.02 ± 0.35	149.59 ± 0.67
$\omega(782)$	1	Eq. ??	781.91 ± 0.24	8.13 ± 0.45
$\rho(1450)$	1	GS	1493 ± 15	427 ± 31
$\rho(1700)$	1	GS	1861 ± 17	316 ± 26
$f_2(1270)$	2	RBW	1275.1 ± 1.2	$185.1 \,^{+\,2.9}_{-\,2.4}$
$\pi\pi$ S-wave	0	K-matrix	See Sec. ??	
$f_0(500)$	0	Eq. ??	See Sec. ??	
$f_0(980)$	0	Eq. ??	See Sec. ??	
$f_0(2020)$	0	RBW	1992 ± 16	442 ± 60
Nonresonant	0	Eq. ??	See Sec. ??	

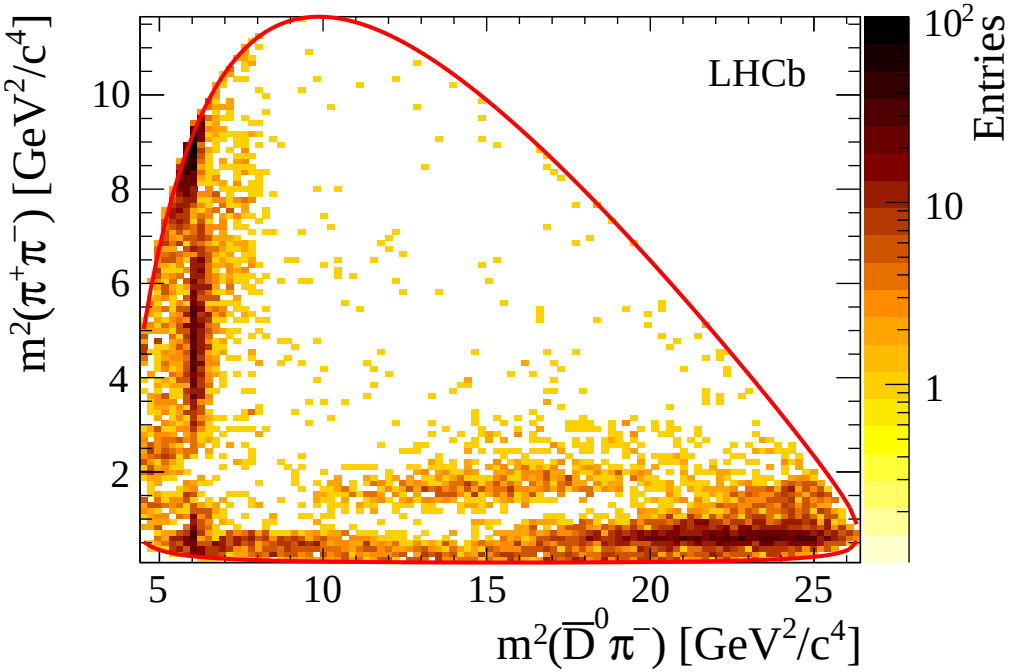

Resonance	Spin	Model	m_r (MeV/c^2)	Γ_0 (MeV)
$\bar{D}^0\pi^-$ P-wave	1	Eq. ??	Floated	
$D_0^*(2400)^-$	0	RBW	Floated	
$D_2^*(2460)^-$	2	RBW	Floated	
$D_J^*(2760)^-$	3	RBW	Floated	
$\rho(770)$	1	GS	775.02 ± 0.35	149.59 ± 0.67
$\omega(782)$	1	Eq. ??	781.91 ± 0.24	8.13 ± 0.45
$\rho(1450)$	1	GS	1493 ± 15	427 ± 31
$\rho(1700)$	1	GS	1861 ± 17	316 ± 26
$f_2(1270)$	2	RBW	1275.1 ± 1.2	$185.1 \pm^{2.9}_{2.4}$
$\pi\pi$ S-wave	0	K-matrix	See Sec. ??	
$f_0(500)$	0	Eq. ??	See Sec. ??	
$f_0(980)$	0	Eq. ??	See Sec. ??	
$f_0(2020)$	0	RBW	1992 ± 16	442 ± 60
Nonresonant	0	Eq. ??	See Sec. ??	

$D_J^*(2760)$:

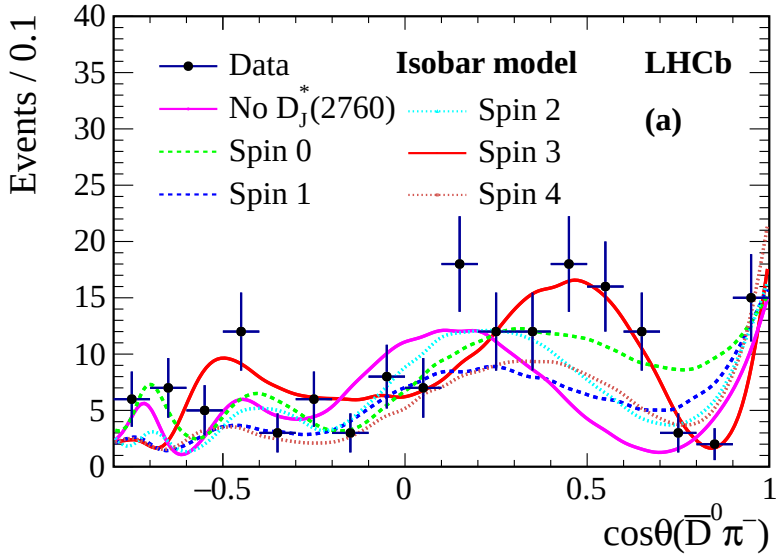

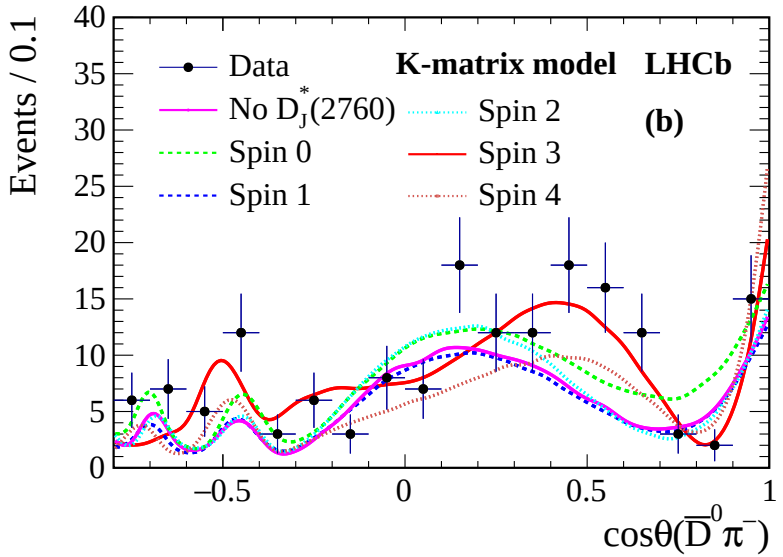

Comparison of isobar and K-matrix for spin-0 $\pi^+\pi^-$ wave

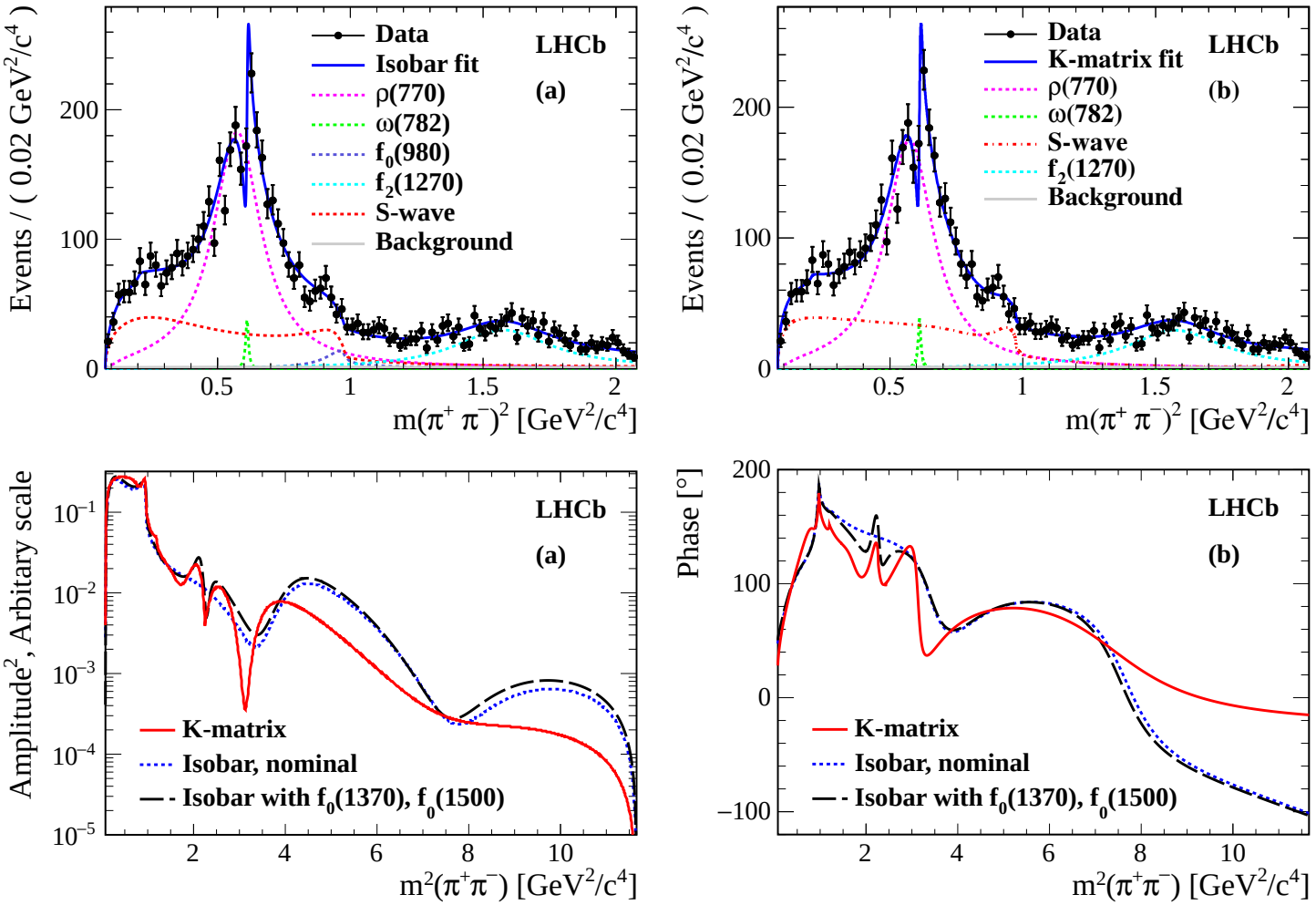

There are differences, but the effect on the fit quality is small.

Model-independent approaches: Legendre moments

Allow to investigate the helicity structure as a function of m^2 *without* performing a fit. Use the fact that partial wave with spin J is a Legendre polynomial $P_J(\cos\theta_{\rm hel})$.

Weight events as functions of helicity:

$$w_i = P_L(\cos\theta_{\rm hel})$$

Partial waves with spins up to J give moments up to $2J$ in the event density.

If we are limited to S, P and D waves:

$$\langle P_0 \rangle = |h_0|^2 + |h_1|^2 + |h_2|^2$$

$$\langle P_1 \rangle = \frac{2}{\sqrt{3}}|h_0||h_1|\cos\delta_{01} + \frac{4}{\sqrt{15}}|h_1||h_2|\cos\delta_{12}$$

$$\langle P_2 \rangle = \frac{2}{\sqrt{5}}|h_0||h_2|\cos\delta_{02} + \frac{2}{5}|h_1|^2 + \frac{2}{7}|h_2|^2$$

$$\langle P_3 \rangle = \frac{6}{7}\sqrt{\frac{3}{5}}|h_1||h_2|\cos\delta_{12}$$

$$\langle P_4 \rangle = \frac{2}{7}|h_2|^2$$

Resonances only in one channel: $D^+\pi^-$: ideal for Legendre polynomial approach

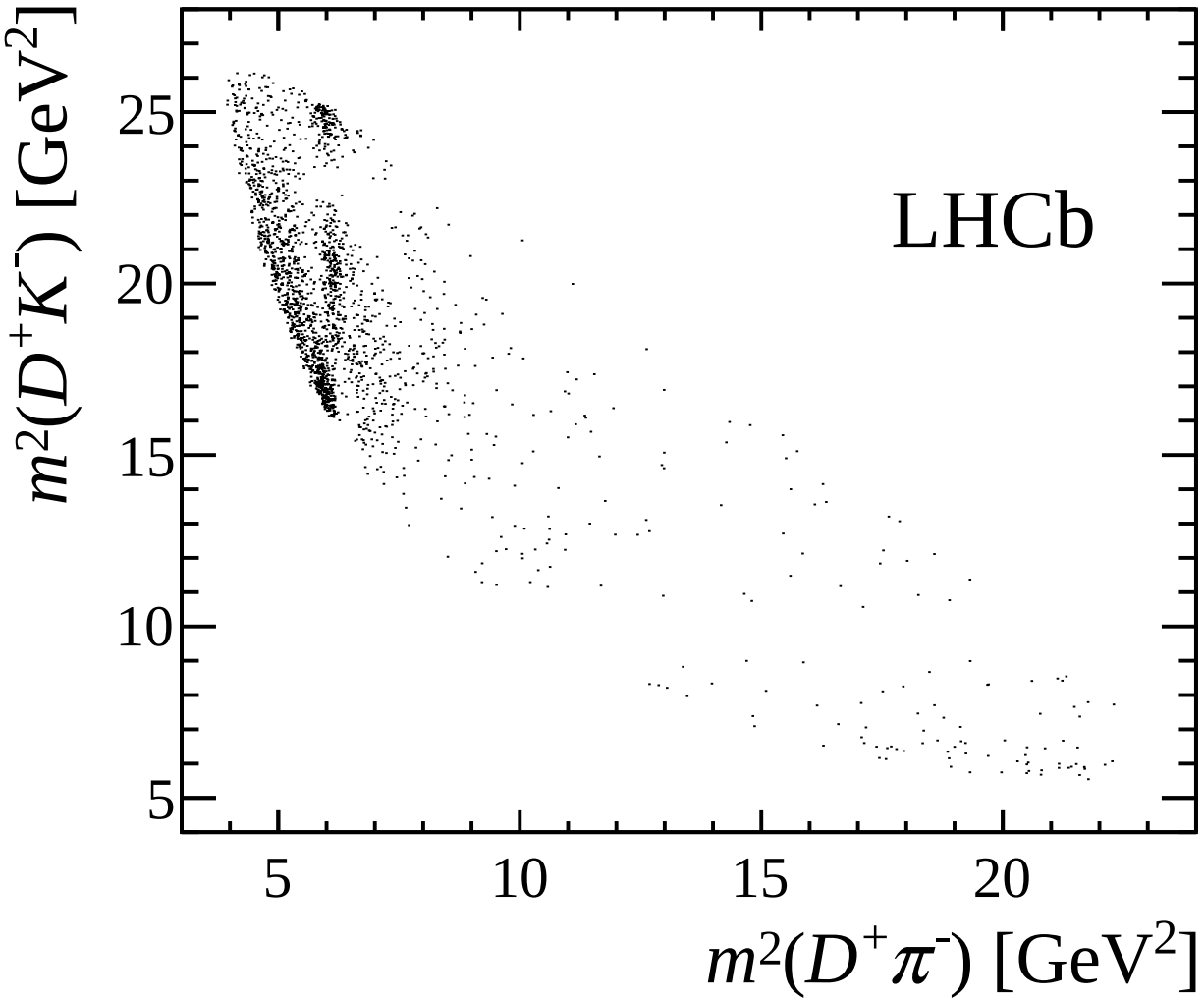

Legendre moments: $B^- \to D^+ K^- \pi^-$ [PRD 91 (2015) 092002]

Consider contributions up to spin-3:

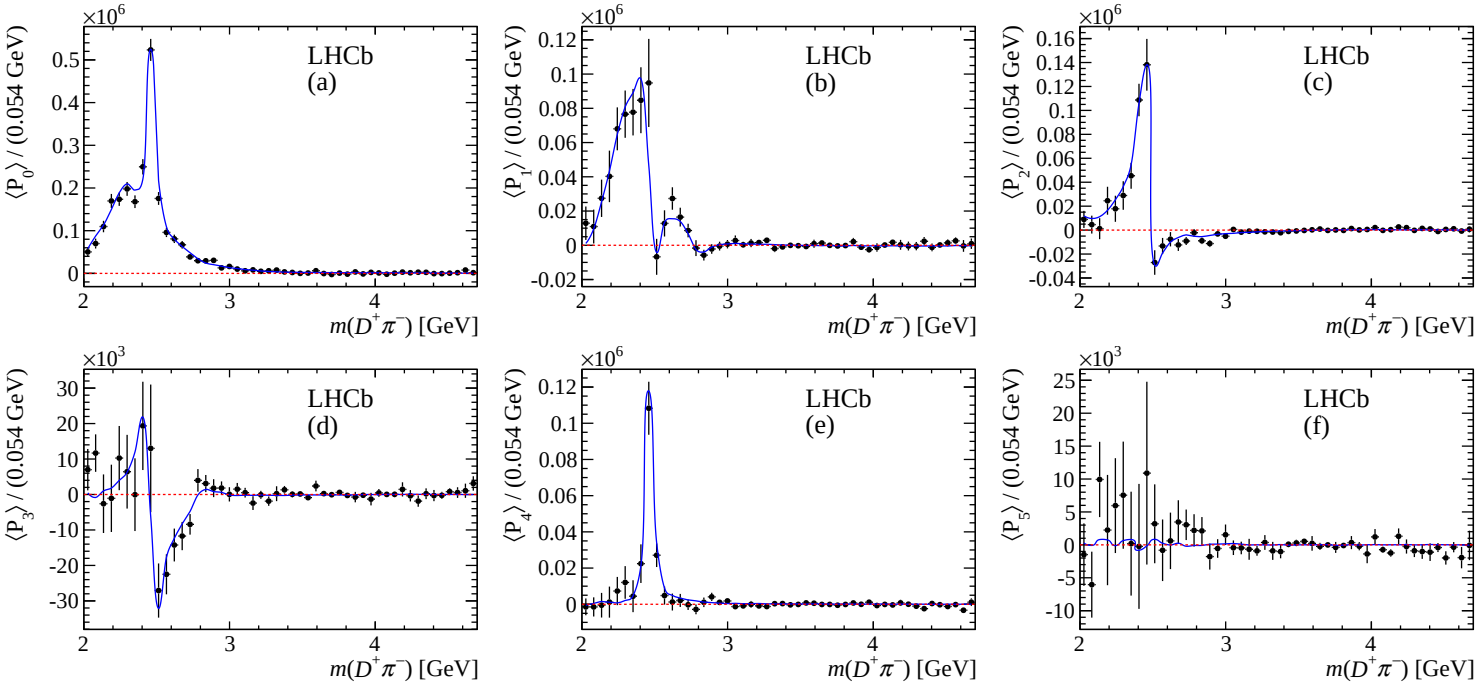

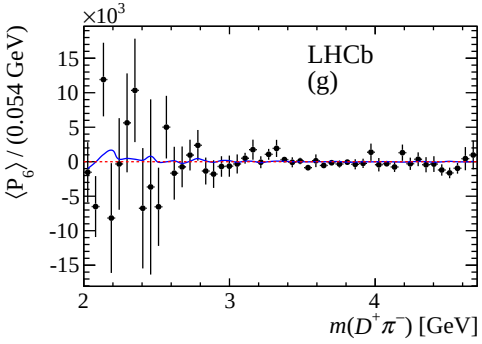

- Moments 6 and 7 consistent with 0: no evidence for PW with spin-3.
- Spin-2 apparent in moment 4: single state $D_2^*(2460)$
- Moment 3 differs from 4: interference with spin-2 and broad spin-1
- Moments 1 and 3 differ again: interference of spin-1 and spin-0 (broad as well)

Resonances only in $D^+\pi^-$, but two identical pions in the final state: need to symmetrise the amplitude

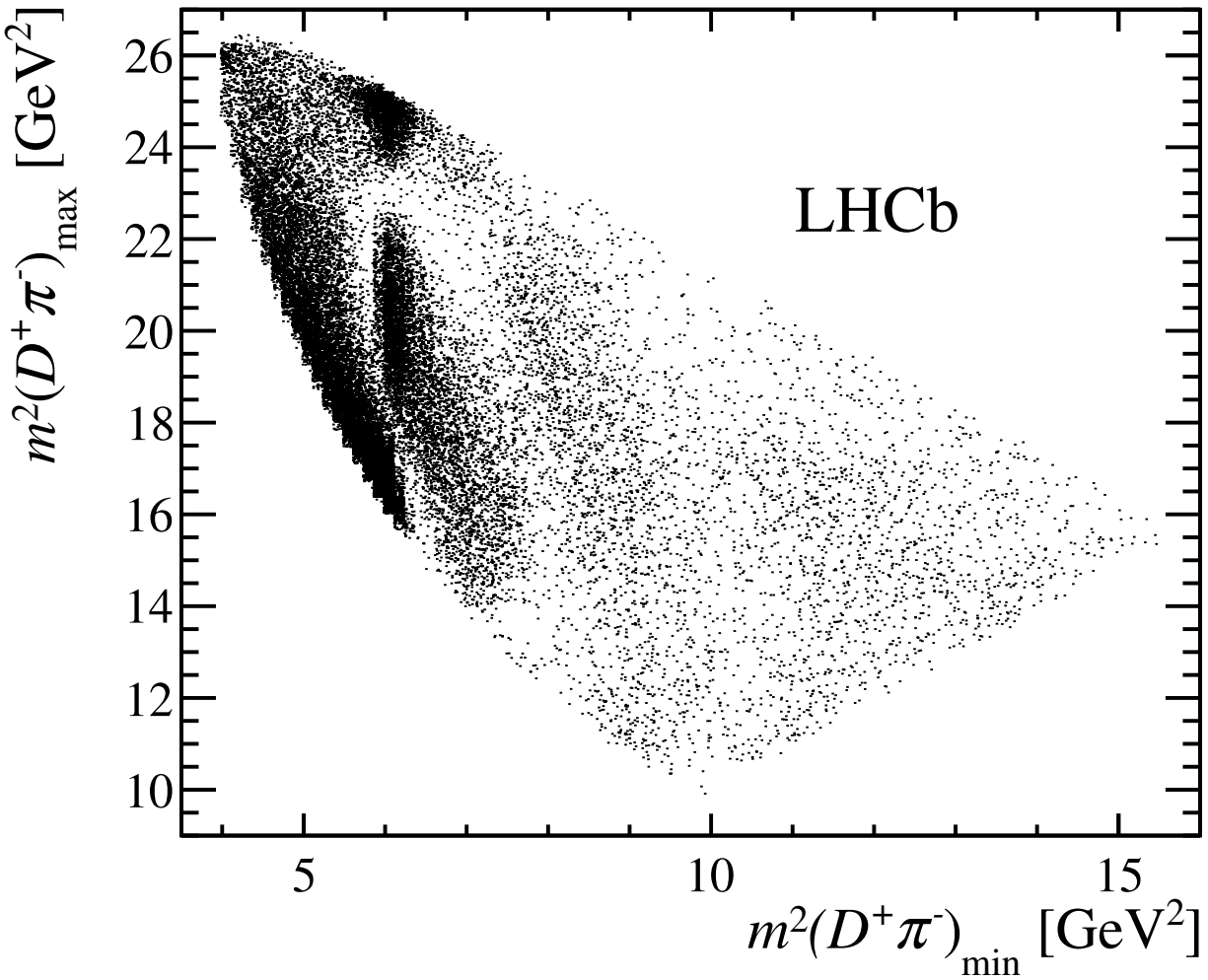

Consider contributions up to spin-3:

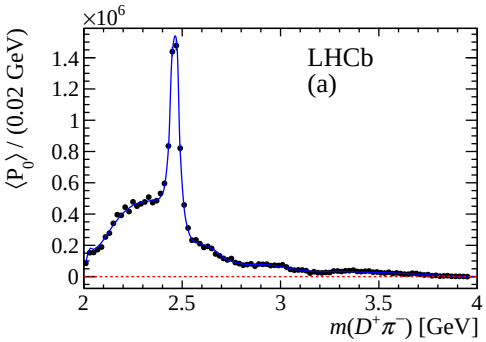

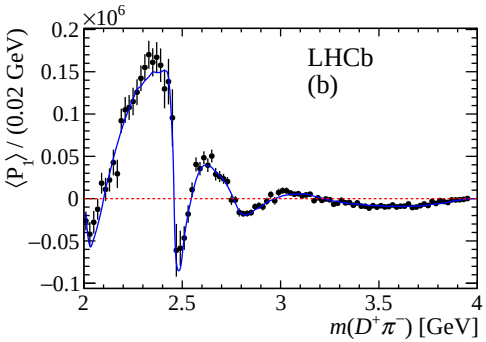

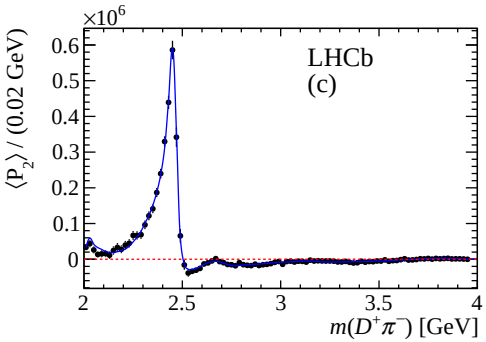

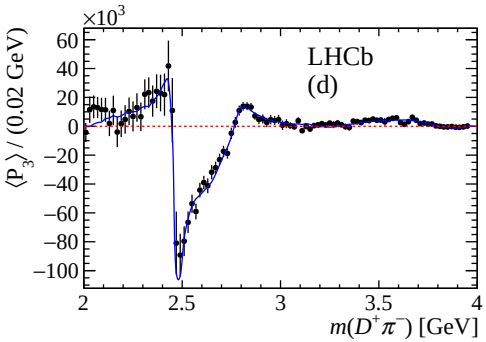

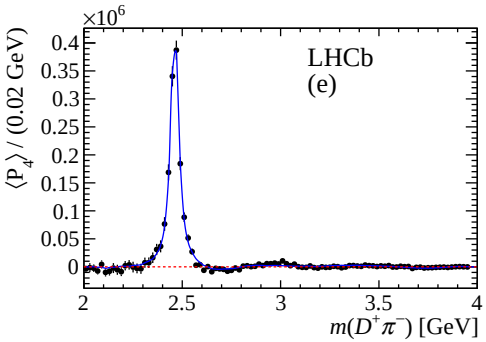

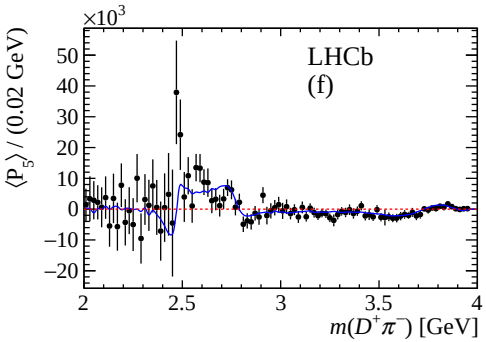

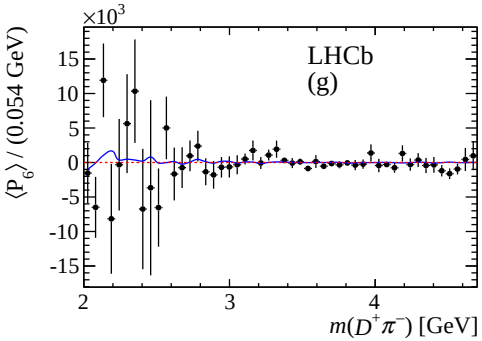

- Some activity in moments 6 and 7: evidence for PW with spin-3.

Large data sample allows to describe the S-wave by a model-independent spline-interpolated shape.
$Re(A)$ and $Im(A)$ in each node are fitted.
Interference with higher-spin waves provides information about the phase.

Resonance	Spin	Model	Parameters
$D_2^*(2460)^0$	2	RBW	Determined from data (see Table **??**)
$D_1^*(2680)^0$	1	RBW	
$D_3^*(2760)^0$	3	RBW	
$D_2^*(3000)^0$	2	RBW	
$D_v^*(2007)^0$	1	RBW	$m = 2006.98 \pm 0.15\,\text{MeV}$, $\Gamma = 2.1\,\text{MeV}$
B_v^{*0}	1	RBW	$m = 5325.2 \pm 0.4\,\text{MeV}$, $\Gamma = 0.0\,\text{MeV}$
Total S-wave	0	MIPW	See text

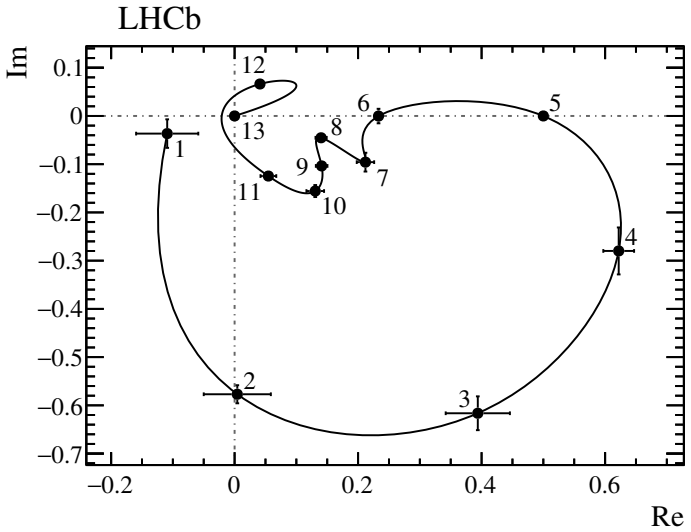

Phase rotation due to resonant $D^*(2400)$ state.

$D^0 \to K^0_S\pi^+\pi^-$ Dalitz plot

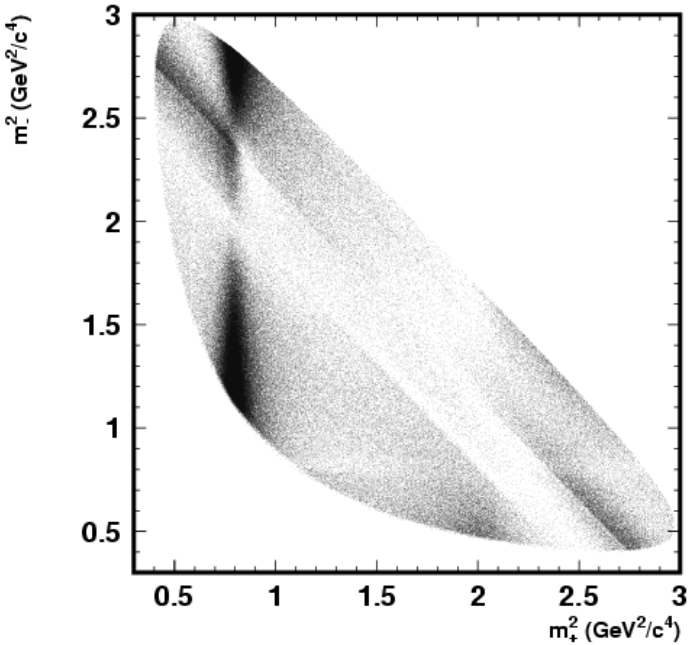

The amplitude contains $O(10)$ resonant contributions in $K\pi$ (K^*, K^*_0, K^*_2) and $\pi\pi$ (ρ, ω, f_0, f_2 etc.) channels

$D^0 \to K^0_S\pi^+\pi^-$ decay is unique to combine the following properties:

- High branching fraction.
- Rich resonance structure $\Rightarrow$ significant phase variations across the phase space.

Can be used to effectively measure the properties of $D^0 - \overline{D}^0$ admixture which appears in a few measurements:

- γ measurement in $B \to DK$
- D^0 mixing and CP violation
- β measurement in $B^0 \to D\pi^0$.

CKM angle γ: $D \to K^0_S\pi^+\pi^-$ decay from $B \to DK$

Measures CKM phase γ at tree level, $\Rightarrow$ SM reference point.

$B^- \to D^0 K^-$:

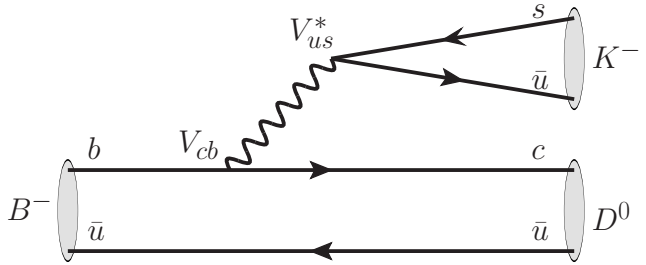

$A \sim V_{cb}V^*_{us} \sim A\lambda^3$

$B^- \to \overline{D}^0 K^-$:

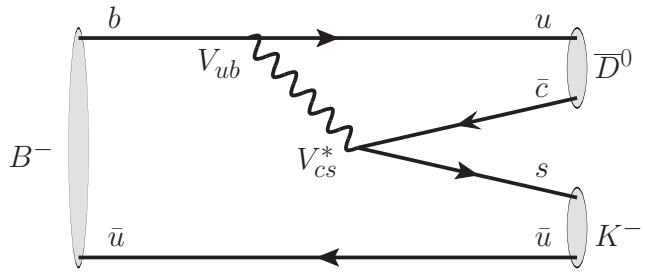

$A \sim V_{ub}V^*_{cs} \sim A\lambda^3(\rho - i\eta)$

If D^0 and $\overline{D}^0$ decay into the same final state: $|\tilde{D}\rangle = |D^0\rangle + r_B e^{\pm i\gamma + i\delta_B}|\overline{D}^0\rangle$ for $B^\pm$

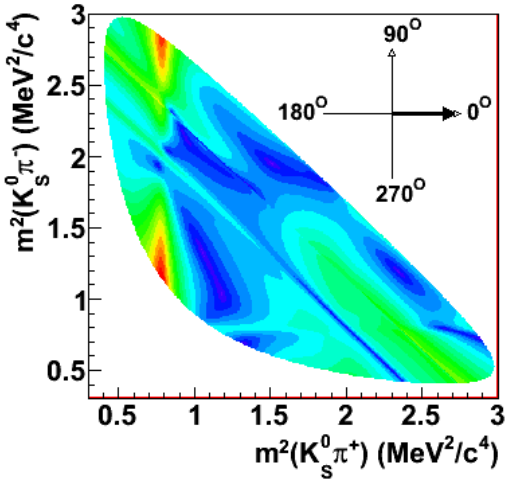

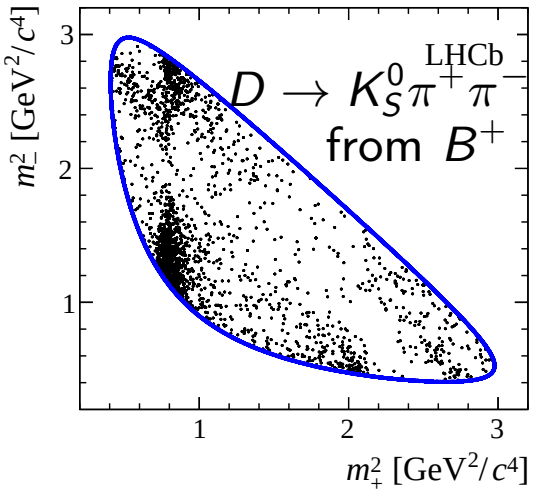

2D kinematic distribution of $D \to K^0_S\pi^+\pi^-$ from $B^\pm \to DK^\pm$

$$p_\pm(m^2_+, m^2_-) = |A_D + r_B e^{\pm i\gamma + i\delta}\,\overline{A}_D|^2$$

where A_D is known from flavour-specific $D^* \to D^0\pi$ decays

Obtain unknown r_B, δ_B and γ.

CKM angle γ: $D \to K^0_S\pi^+\pi^-$ decay from $B \to DK$

Measures CKM phase γ at tree level, $\Rightarrow$ SM reference point.

$B^- \to D^0 K^-$:

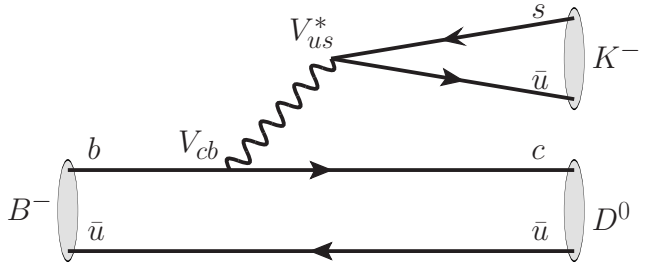

$A \sim V_{cb}V^*_{us} \sim A\lambda^3$

$+$

$B^- \to \overline{D}^0 K^-$:

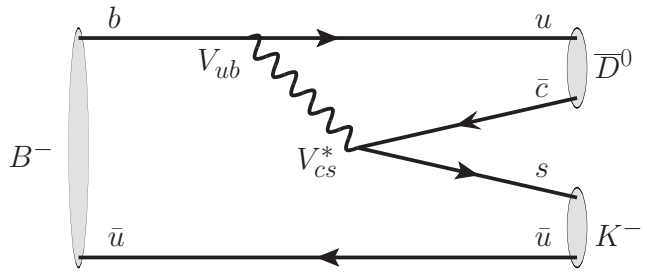

$A \sim V_{ub}V^*_{cs} \sim A\lambda^3(\rho - i\eta)$

If D^0 and $\overline{D}^0$ decay into the same final state: $|\tilde{D}\rangle = |D^0\rangle + r_B e^{\pm i\gamma + i\delta_B}|\overline{D}^0\rangle$ for $B^\pm$

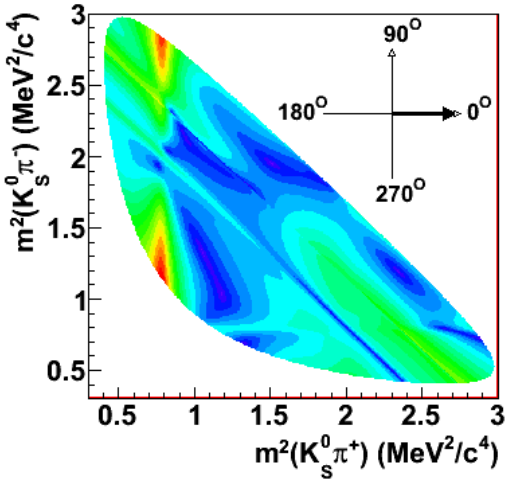

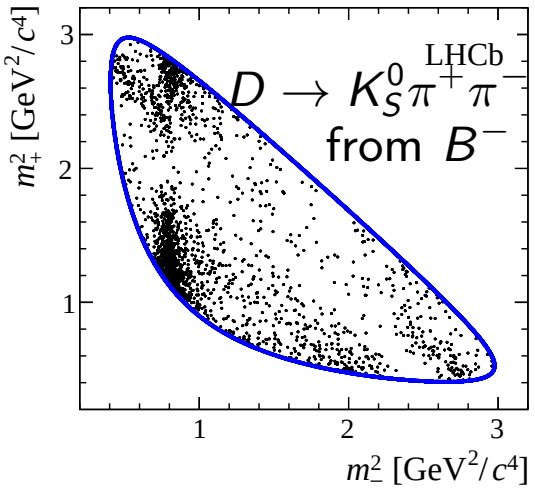

2D kinematic distribution of $D \to K^0_S\pi^+\pi^-$ from $B^\pm \to DK^\pm$

$$p_\pm(m^2_+, m^2_-) = |A_D + r_B e^{\pm i\gamma + i\delta}\,\overline{A}_D|^2$$

where A_D is known from flavour-specific $D^* \to D^0\pi$ decays

Obtain unknown r_B, δ_B and γ.

Time-dependent Dalitz plot analysis: charm mixing

[Belle, PRL 99, 131803 (2007)]

Measure D^0 oscillations using $D^0 \to K^0_S \pi^+ \pi^-$:

$$\mathcal{A}(m^2_+, m^2_-) = \mathcal{A}_D(m^2_+, m^2_-)(e^{-i\lambda_1 t} + e^{-i\lambda_2 t}) + \frac{q}{p}\mathcal{A}_D(m^2_-, m^2_+)(e^{-i\lambda_1 t} - e^{-i\lambda_2 t})$$

where $\lambda_{1,2} = \lambda_{1,2}(x, y)$

Provides direct measurement of x and y.

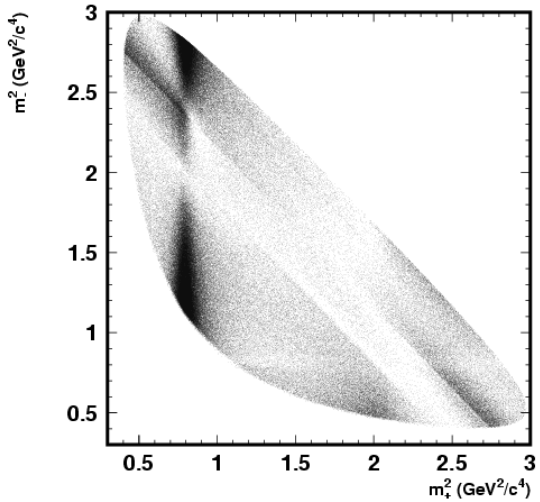

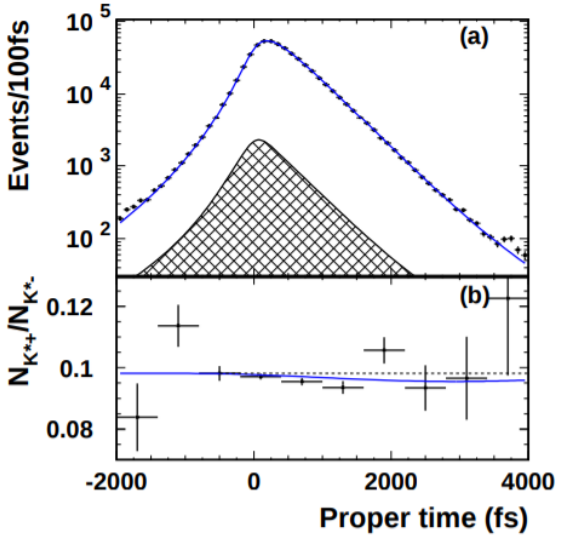

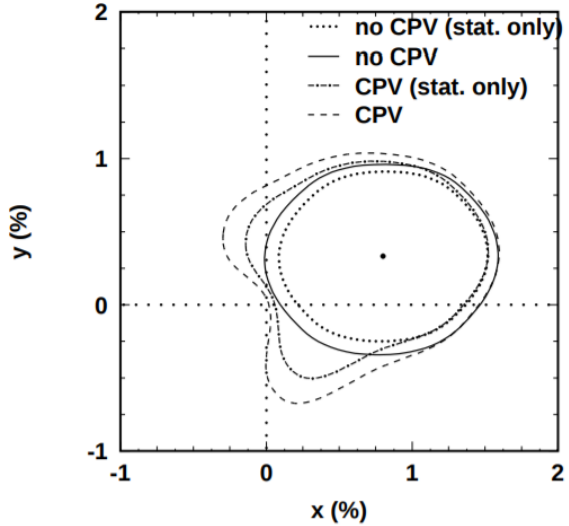

Part II
Multidimensional amplitude analyses

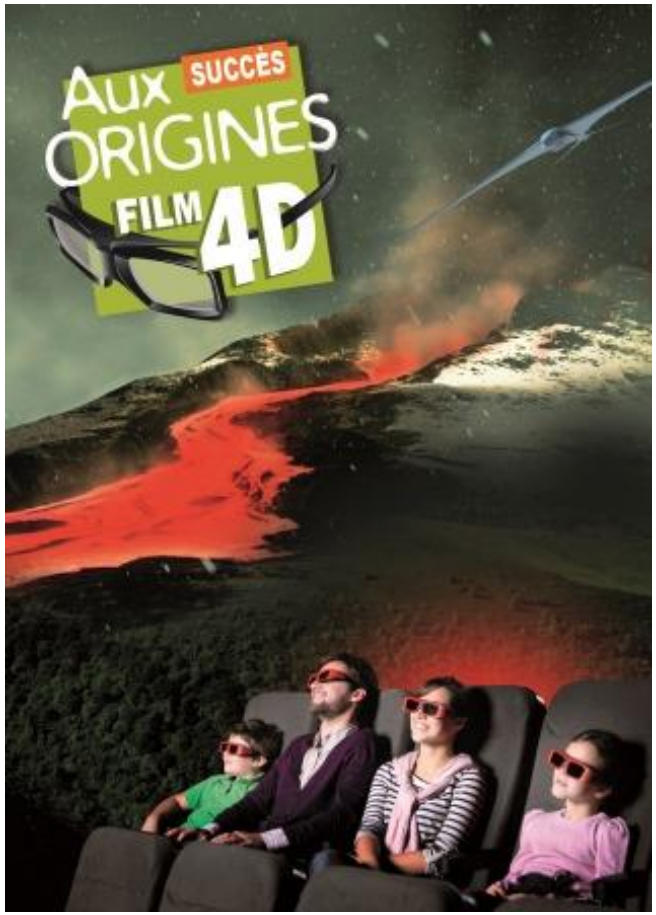

Going beyond 2D: multibody decays and non-scalar initial/final states

N-body decay into scalars: $3N - 7$ internal degrees of freedom.
4-body: 5D phase space.

[LHCb, EPJC 78 (2018) 443]

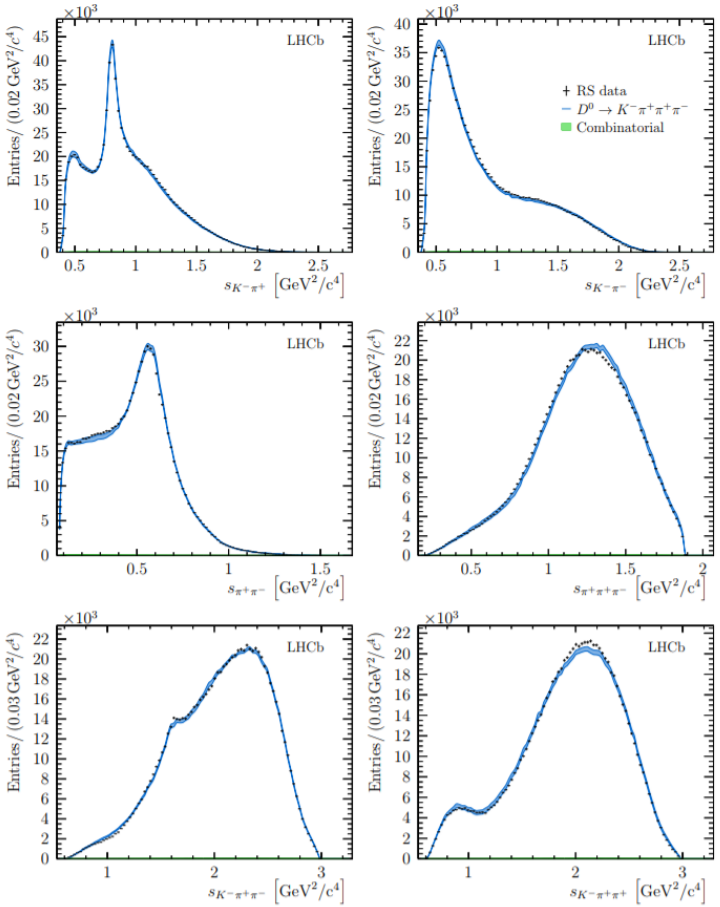

	Fit Fraction [%]	$\lvert g\rvert$	$\arg(g)[^o]$
$\left[\overline{K}^*(892)^0\rho(770)^0\right]^{L=0}$	$7.34 \pm 0.08 \pm 0.47$	$0.196 \pm 0.001 \pm 0.015$	$-22.4 \pm 0.4 \pm 1.6$
$\left[\overline{K}^*(892)^0\rho(770)^0\right]^{L=1}$	$6.03 \pm 0.05 \pm 0.25$	$0.362 \pm 0.002 \pm 0.010$	$-102.9 \pm 0.4 \pm 1.7$
$\left[\overline{K}^*(892)^0\rho(770)^0\right]^{L=2}$	$8.47 \pm 0.09 \pm 0.67$		
$\left[\rho(1450)^0\overline{K}^*(892)^0\right]^{L=0}$	$0.61 \pm 0.04 \pm 0.17$	$0.162 \pm 0.005 \pm 0.025$	$-86.1 \pm 1.9 \pm 4.3$
$\left[\rho(1450)^0\overline{K}^*(892)^0\right]^{L=1}$	$1.98 \pm 0.03 \pm 0.33$	$0.643 \pm 0.006 \pm 0.058$	$97.3 \pm 0.5 \pm 2.8$
$\left[\rho(1450)^0\overline{K}^*(892)^0\right]^{L=2}$	$0.46 \pm 0.03 \pm 0.15$	$0.649 \pm 0.021 \pm 0.105$	$-15.6 \pm 2.0 \pm 4.1$
$\rho(770)^0\left[K^-\pi^+\right]^{L=0}$	$0.93 \pm 0.03 \pm 0.05$	$0.338 \pm 0.006 \pm 0.011$	$73.0 \pm 0.8 \pm 4.0$
$\alpha_{3/2}$		$1.073 \pm 0.008 \pm 0.021$	$-130.9 \pm 0.5 \pm 1.8$
$\overline{K}^*(892)^0\left[\pi^+\pi^-\right]^{L=0}$	$2.35 \pm 0.09 \pm 0.33$		
$f_{\pi\pi}$		$0.261 \pm 0.005 \pm 0.024$	$-149.0 \pm 0.9 \pm 2.7$
β_1		$0.305 \pm 0.011 \pm 0.046$	$65.6 \pm 1.5 \pm 4.0$
$a_1(1260)^+K^-$	$38.07 \pm 0.24 \pm 1.38$	$0.813 \pm 0.006 \pm 0.025$	$-149.2 \pm 0.5 \pm 3.1$
$K_1(1270)^-\pi^+$	$4.66 \pm 0.05 \pm 0.39$	$0.362 \pm 0.004 \pm 0.015$	$114.2 \pm 0.8 \pm 3.6$
$K_1(1400)^-\left[\overline{K}^*(892)^0\pi^-\right]\pi^+$	$1.15 \pm 0.04 \pm 0.20$	$0.127 \pm 0.002 \pm 0.011$	$-169.8 \pm 1.1 \pm 5.9$
$K_2^*(1430)^-\left[\overline{K}^*(892)^0\pi^-\right]\pi^+$	$0.46 \pm 0.01 \pm 0.03$	$0.302 \pm 0.004 \pm 0.011$	$-77.7 \pm 0.7 \pm 2.1$
$K(1460)^-\pi^+$	$3.75 \pm 0.10 \pm 0.37$	$0.122 \pm 0.002 \pm 0.012$	$172.7 \pm 2.2 \pm 8.2$
$\left[K^-\pi^+\right]^{L=0}\left[\pi^+\pi^-\right]^{L=0}$	$22.04 \pm 0.28 \pm 2.09$		
$\alpha_{3/2}$		$0.870 \pm 0.010 \pm 0.030$	$-149.2 \pm 0.7 \pm 3.5$
$\alpha_{K\eta'}$		$2.614 \pm 0.141 \pm 0.281$	$-19.1 \pm 2.4 \pm 12.0$
β_1		$0.554 \pm 0.009 \pm 0.053$	$35.3 \pm 0.7 \pm 1.6$
$f_{\pi\pi}$		$0.082 \pm 0.001 \pm 0.008$	$-147.0 \pm 0.7 \pm 2.2$
Sum of Fit Fractions	$98.29 \pm 0.37 \pm 0.84$		
χ^2/ν	$40483/32701 = 1.238$		

$D^0 \to K^+\pi^-\pi^+\pi^-$ and $D^0 \to K^-\pi^+\pi^-\pi^+$ decays.
Can be used for γ measurement in $B \to DK$, charm mixing, etc.

Going beyond 2D: multibody decays and non-scalar initial/final states

Non-scalar particle in the final state adds more degrees of freedom to the 2D 3-body phase space

Examples:

- $B^0 \to \psi' \pi^- K^+$, $\psi' \to \mu^+ \mu^-$: 4 variables in the phase space

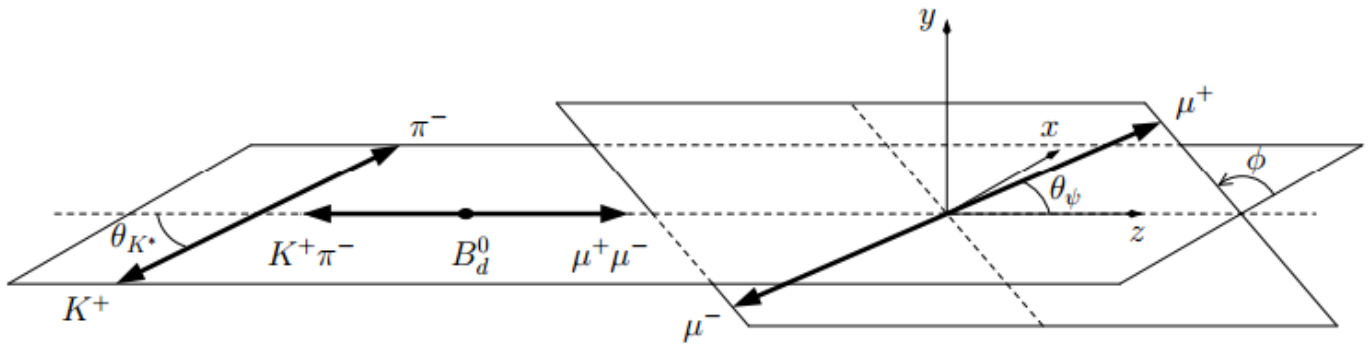

- $B^+ \to J/\psi \phi K^+$, $J/\psi \to \mu^+ \mu^-$, $\phi \to K^+ K^-$: 6 variables in the phase space

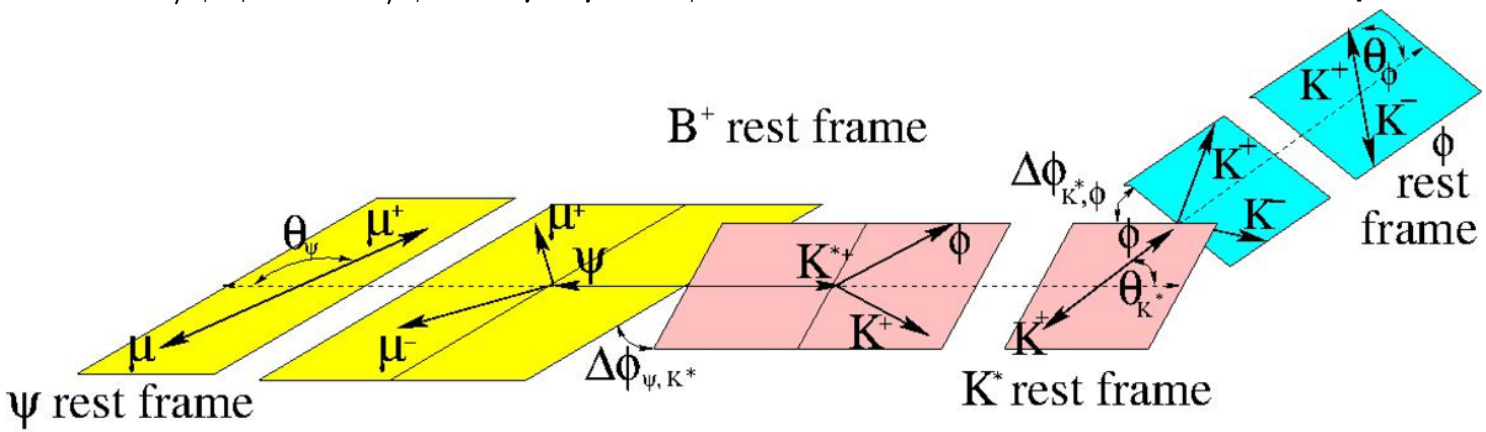

[S.-U. Chung, Spin formalisms]

[R. Kutschke, An angular distribution cookbook]

Rotations of one-particle states

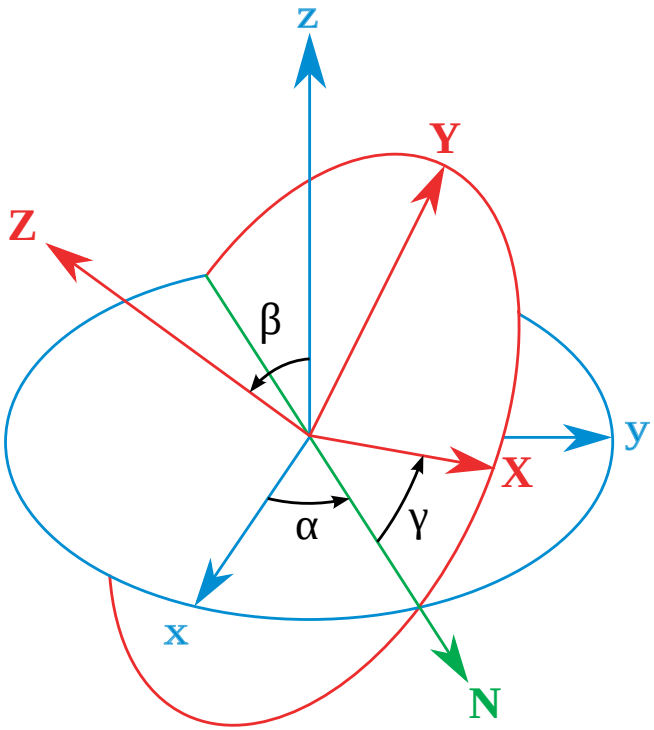

Definition of Euler angles (ZYZ convention)

Basis of states with spin J and projection m

$$|Jm\rangle$$

Transformation after rotation of coordinate system $(\hat{x}, \hat{y}, \hat{z}) \to (\hat{x}', \hat{y}', \hat{z}')$

$$|Jm'\rangle = \sum_{mm'} D^J_{m,m'}(\alpha, \beta, \gamma)|Jm\rangle,$$

where α, β, γ are Euler angles (ZYZ convention), Wigner D matrix

$$D^J_{mm'}(\alpha, \beta, \gamma) = e^{-im\alpha} d^J_{m,m'}(\beta) e^{-im'\gamma},$$

and Wigner small-d is a combination of sin and cos of β:

$d^{1/2}_{1/2,1/2} = \cos(\beta/2)$	$d^1_{1,1} = \frac{1}{2}(1+\cos\beta)$	$d^1_{0,0} = \cos\beta$
$d^{1/2}_{1/2,-1/2} = -\sin(\beta/2)$	$d^1_{1,-1} = \frac{1}{2}(1-\cos\beta)$	$d^1_{1,0} = -\frac{1}{\sqrt{2}}\sin\beta$

Two-body decays

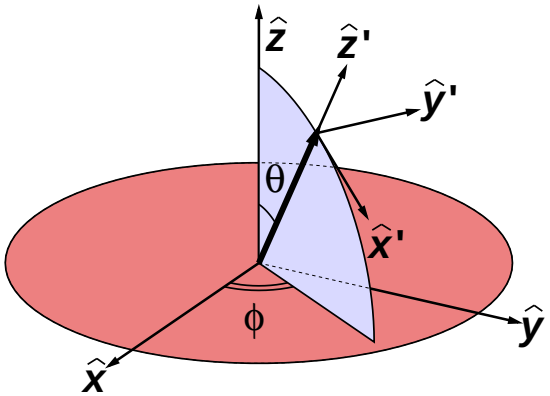

Transformation of coordinates to helicity frame

Decay $A \to BC$: $\vec{p}_A = \vec{p}_B + \vec{p}_C$

Helicity basis: state defined by projection λ of its spin onto momentum $\vec{p}$.

Project two-particle state BC onto one-particle A.

Initial frame: rest frame of A.

Rotation to helicity frame (angles θ, ϕ) aligned with breakup momentum $\vec{p}_B = -\vec{p}_C$:

Coupling of initial $|J_A m_A\rangle$ to final $|J_B \lambda_B\rangle|J_C \lambda_C\rangle$:

$$\mathcal{A}_{\lambda_B,\lambda_C} D^{j_A}_{m_A,\lambda_B-\lambda_C}(\phi,\theta,0)^* = \mathcal{A}_{\lambda_B,\lambda_C} e^{i m_A \phi} d^{J_A}_{m_A,\lambda_B-\lambda_C}(\theta)$$

(the last rotation around $\hat{z}'$ is arbitraty, here we have $\gamma = 0$, alternatively could have $\gamma = -\phi$)

Sequential decays

Decay $A \to BC$, $B \to DE$, ...: sequence of rotations and boosts to the rest frame of each intermediate resonance.

- Start with A rest frame.
- Rotate to BC helicity frame. Corresponding spin factor

$$\mathcal{A}_{\lambda_B,\lambda_C} e^{i m_A \phi_{BC}} d^{J_A}_{m_A,\lambda_B-\lambda_C}(\theta_{BC})$$

- Boost to B rest frame.
- Rotate to DE helicity frame. Spin factor

$$\times \mathcal{A}_{\lambda_D,\lambda_E} e^{i \lambda_B \phi_{DE}} d^{J_B}_{\lambda_B,\lambda_D-\lambda_E}(\theta_{DE})$$

  (note that $(\phi, \theta)_{DE}$ are defined in the B rest frame).
- ... Continue until final state particles are reached

$\Lambda_b^0 \to J/\psi \Lambda^*$, $J/\psi \to \mu^+\mu^-$, $\Lambda^* \to p\pi$:

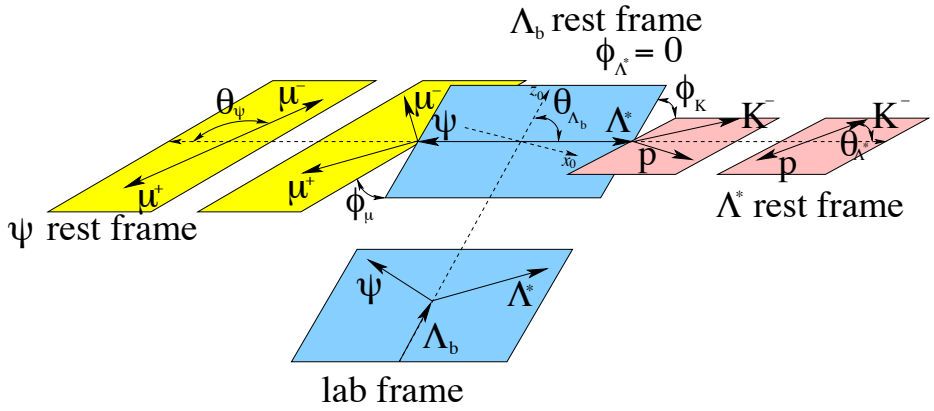

Parity conservation

- Each quasi-two-body decay $A \to BC$ is accompanied by a set of (complex) coupling constants $\mathcal{A}_{\lambda_1,\lambda_2}$, which are typically free parameters of the amplitude fit.
- Parity conservation provides additional constraints if B, C are not scalars:

$$\mathcal{A}_{-\lambda_B,-\lambda_C} = P_A P_B P_C (-1)^{J_B+J_C-J_A} \mathcal{A}_{\lambda_B,\lambda_C}$$

  ($P_{A,B,C}$ are parities of the states)
- This:
  - Reduces the number of free parameters
  - Provides sensitivity to parities of intermediate resonances.
- Does not work for weak decays (first decay in the sequence for weakly-decaying particles): need to fit $\mathcal{A}_{-\lambda_B,-\lambda_C}$ and $\mathcal{A}_{\lambda_B,\lambda_C}$ separately.

Non-scalar initial state

With non-scalar initial states (e.g. for decays of baryons), one has to take possible initial polarisation into account.
Rotation of the rest frame of the initial particle is, in principle, arbitrary. Two common choices:

- Use the frame inspired by the possible polarisation of the initial particle. E.g. for $\Lambda_b^0 \to D^0 p \pi^-$: $\hat{z}$ is perpendicular to production plane.

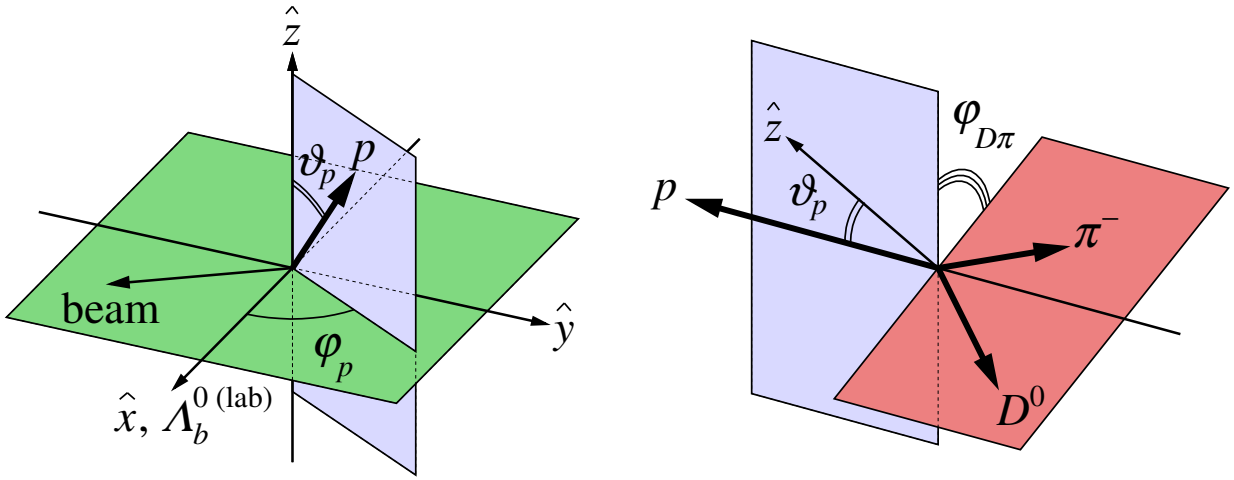

  Three-body decay is fully determined by 5 variables $m^2_{Dp}, m^2_{p\pi}, \vartheta_p, \varphi_p, \varphi_{D\pi}$

- Helicity frame: $\hat{z}$ along $\vec{p}_A$ in lab. frame (e.g. pentaquark analyses). Forget about polarisation (longitudinal Λ_b^0 polarisation is forbidden by strong production mechanisms), assume Λ_b^0 unpolarised.

In practice, the polarisation of Λ_b^0 is small, so can be ignored in many cases.

Spin-orbital couplings

Coupling constants $\mathcal{A}_{\lambda_B,\lambda_C}$ correspond to definite helicities of the final state particles. It might be useful to use spin-orbital ($\mathcal{B}_{L,S}$) couplings instead:

$$\mathcal{A}_{\lambda_B,\lambda_C} = \sum_L \sum_S \sqrt{\frac{2L+1}{2J_A+1}} \left(\begin{array}{cc|c} J_B & J_C & S \\ \lambda_B & -\lambda_C & \lambda_B - \lambda_C \end{array} \right) \left(\begin{array}{cc|c} L & S & J_A \\ 0 & \lambda_B - \lambda_C & \lambda_B - \lambda_C \end{array} \right) \times \mathcal{B}_{L,S}$$

- Breit-Wigner corrections depend on definite orbital momentum L (Blatt-Weisskopf FF, mass-dependent width)
- Limit L to only lowest possible values to reduce the number of free parameters

Spin alignment of final-state particles

Consider we have different decay sequences (e.g. Λ_b^0) leading to the same final state (e.g. $Dp\pi$):

$\Lambda_b^0 \to \Lambda_c^* \pi$, $\Lambda_c^* \to Dp$ and $\Lambda_b \to DN^*$, $N^* \to p\pi^-$

Helicities of the final state particles are defined in different frames (e.g. for p it's either Dp or $p\pi$ rest frame).

Before we can sum up the amplitudes incoherently over the final state polarisations, we need to make sure they are defined consistently in the same frame.

Again, familiar rotation:

$$|\lambda\rangle = \sum_{\lambda'} D(\phi, \theta, \psi)|\lambda'\rangle,$$

where ϕ, θ, ψ are the Euler angles rotating the frame of the "other" decay chain into the chosen "reference" polarisation frame (in the rest frame of the polarised final-state paricle, e.g. p).

Alternatively to helicity formalism which involves Lorentz transformations between different frames, one can use fully covariant expressions.

Covariant tensor formalism: covariant amplitudes expressed via projection operators

$$M_1 = (p_D + p_A)^{\mu} \cdot P^{(1)}_{\mu\nu}(p_B + p_C) \cdot (p_B - p_C)^{\nu}$$

$$M_2 = (p_D + p_A)^{\mu_1}(p_D + p_A)^{\mu_2} \cdot P^{(2)}_{\mu_1\mu_2\nu_1\nu_2}(p_B + p_C) \cdot (p_B - p_C)^{\nu_1}(p_B - p_C)^{\nu_2}$$

where projection operators are direct products of polarisation vectors:

$$P^{(J)}_{\mu_1\ldots\mu_n,\nu_1\ldots\nu_n} = \sum_m e_{\mu_1\ldots\mu_n}(p,m)e^*_{\nu_1\ldots\nu_n}(p,m)$$

Much heavier computationally (need to evaluate multidimensional Lorentz tensors), especially for higher spins, and half-interger spins (additional 4-spinor indices)

Putting it all together (example: $\Lambda_b^0 \to D^0 p\pi^-$)

[JHEP 1705 (2017) 030]

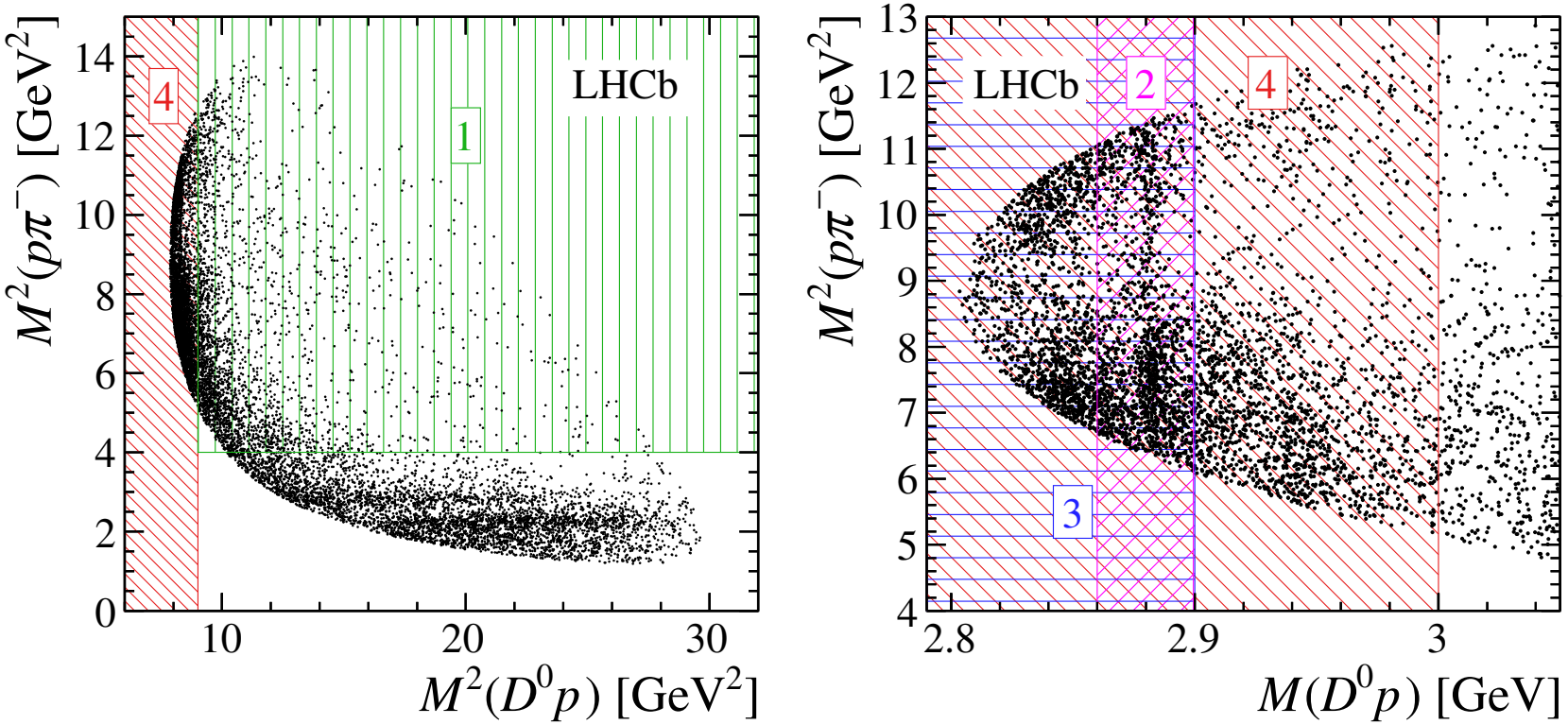

Resonances in D^0p (Λ_c^*) and in $p\pi$ (N^*) channels

D^0p states:

- $\Lambda_c^*(2880)$ ($J^P = 5/2^+$)
- $\Lambda_c^+(2940)$
- Newly observed $\Lambda_c^*(2860)$ ($J^P = 3/2^+$)

Putting it all together (example: $\Lambda_b^0 \to D^0 p\pi^-$)

- $D^0 p$ decay chain (sum up coherently over intermediate resonances and their helicities)

$$A^{(D^0 p)}_{\mu,\lambda_p}(\Omega) = e^{i(\mu\phi_R - \lambda_p\phi_p)} \sum_j \eta_{j,\lambda_p} \left[a_j^+ \, d^{J_{\Lambda_b^0}}_{\mu,+1/2}(\theta_R) \, d^{J_{R_i}}_{+1/2,\lambda_p}(\theta_p) \, \mathcal{R}_j(M^2(D^0 p)) + \right.$$
$$\left. a_j^- \, d^{J_{\Lambda_b^0}}_{\mu,-1/2}(\theta_R) \, d^{J_{R_i}}_{-1/2,\lambda_p}(\theta_p) \, \mathcal{R}_j(M^2(D^0 p)) \, e^{i(\phi_R - \phi_p)} \right] .$$

- $p\pi$ decay chain (taking into account rotation of the proton helicity states)

$$A^{(p\pi^-)}_{\mu,\lambda_p}(\Omega) = \sum_{\lambda'_p = \pm 1/2} d^{1/2}_{\lambda_p,\lambda'_p}(\theta_{\rm rot}) \, e^{i(\mu\phi'_R - \lambda'_p\phi'_p)} \sum_j \eta_{j,\lambda'_p} \times$$
$$\left[a_j^+ \, d^{J_{\Lambda_b^0}}_{\mu,+1/2}(\theta'_R) \, d^{J_{R_i}}_{+1/2,\lambda'_p}(\theta'_p) \, \mathcal{R}_j(M^2(p\pi^-)) + \right.$$
$$\left. a_j^- \, d^{J_{\Lambda_b^0}}_{\mu,-1/2}(\theta'_R) \, d^{J_{R_i}}_{-1/2,\lambda'_p}(\theta'_p) \, \mathcal{R}_j(M^2(p\pi^-)) \, e^{i(\phi'_R - \phi'_p)} \right] ,$$

where

$$\cos\theta_{\rm rot} = \frac{(\vec{p}^{\,(p)}_{\pi^-} \cdot \vec{p}^{\,(p)}_{D^0})}{|\vec{p}^{\,(p)}_{\pi^-}||\vec{p}^{\,(p)}_{D^0})|} ,$$

Putting it all together (example: $\Lambda_b^0 \to D^0 p\pi^-$)

Note we only needed to match p helicities in $D^0 p$ and $p\pi^-$ using a single rotation angle $\theta_{\rm rot}$ since all the decay products are in the same plane.

For more complicated 4-body decays, need to consider both polar and azimuthal angles.

Now we can sum up incoherently over the initial and final state polarisations

$$p(\Omega, P_z) = \sum_{\mu,\lambda_p=\pm 1/2} (1 + 2\mu P_z) \left| A^{(D^0 p)}_{\mu,\lambda_p}(\Omega) + A^{(p\pi^-)}_{\mu,\lambda_p}(\Omega) \right|^2 .$$

P_z is a (possible) polarisation of Λ_b^0 which in practice can be ignored.

Non-scalars in the final state: $B^0 \to \psi' \pi^- K^+$ [PRL 112 (2014) 222002]

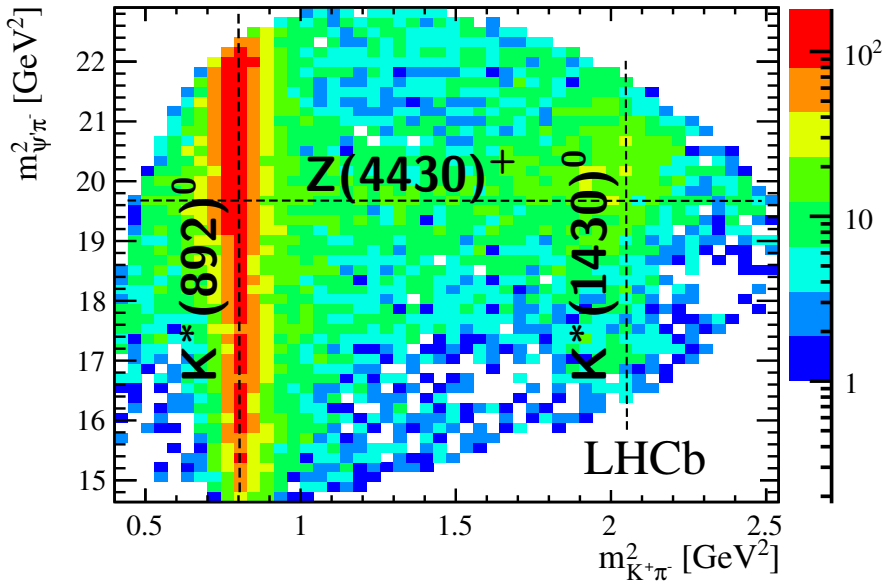

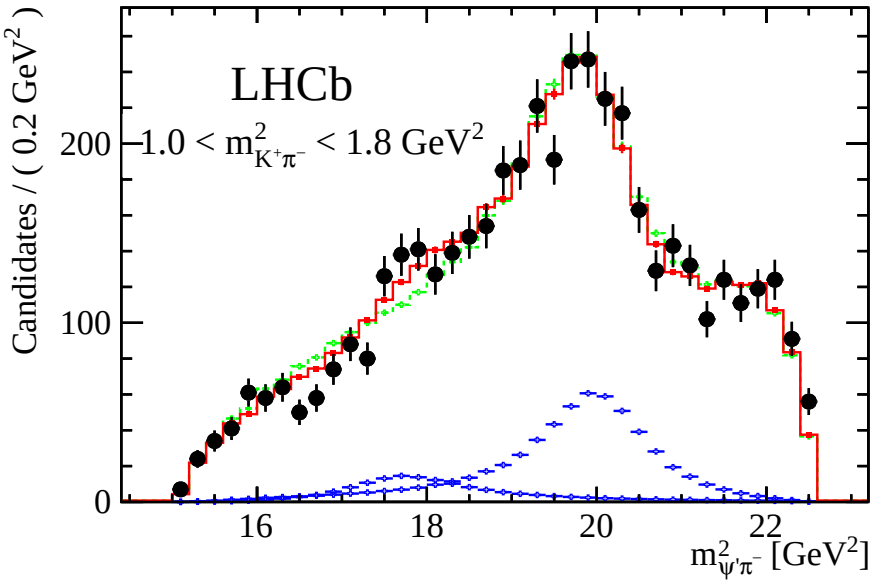

- K^* resonances: $K_0^*(800)$, $K^*(892)$, $K^*(1410)$, $K_{0,2}^*(1430)$, $K^*(1680)$
- Z states:
  - $J^P = 1^+$, 14σ:
    $M = 4475 \pm 7^{+15}_{-25}$ MeV/c^2,
    $\Gamma = 172 \pm 13^{+37}_{-34}$ MeV
  - $J^P = 0^-$, 6σ:
    $M = 4239 \pm 18^{+45}_{-10}$ MeV/c^2,
    $\Gamma = 220 \pm 47^{+108}_{-74}$ MeV

Non-scalars in the final state: $B^0 \to \psi' \pi^- K^+$ [PRL 112 (2014) 222002]

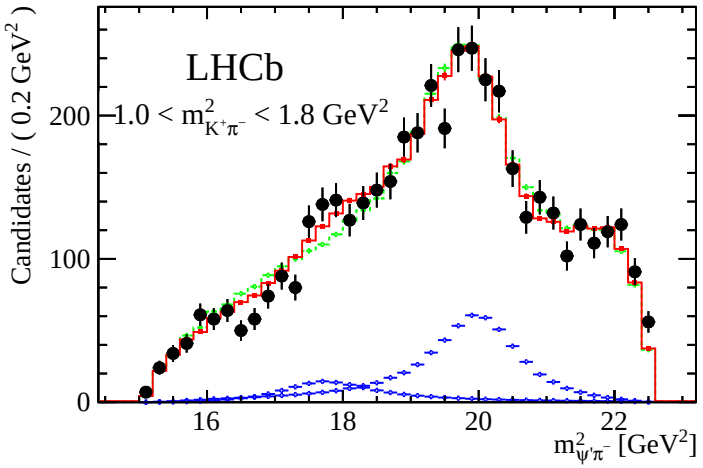

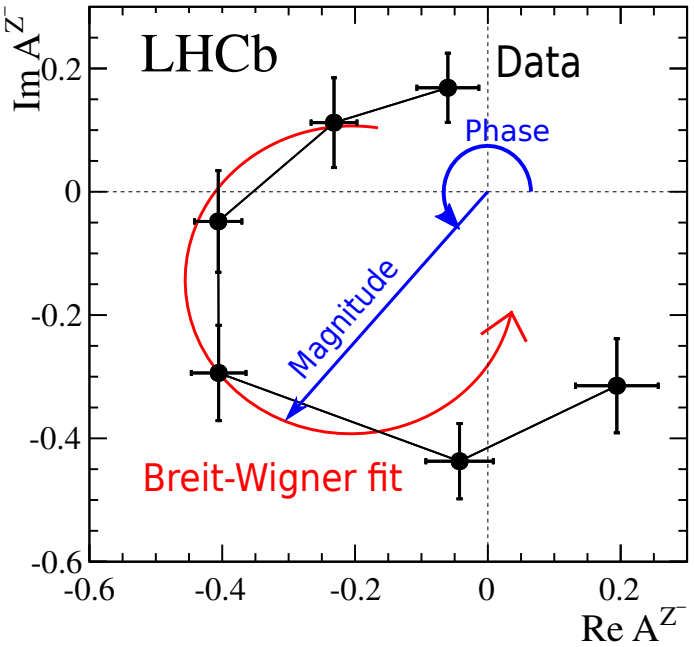

- Model-independent confirmation of phase rotation in $\psi' \pi^-$ amplitude: Argand plot with 6 bins in the range $18 < m^2(\psi' \pi^-) < 21.5\,\mathrm{GeV}/c^2$.
- $Re(A)$ and $Im(A)$ floated independently in each bin
- Interference with the $K^- \pi^+$ amplitude provides access to the phase

First 6 normalised Legendre moments

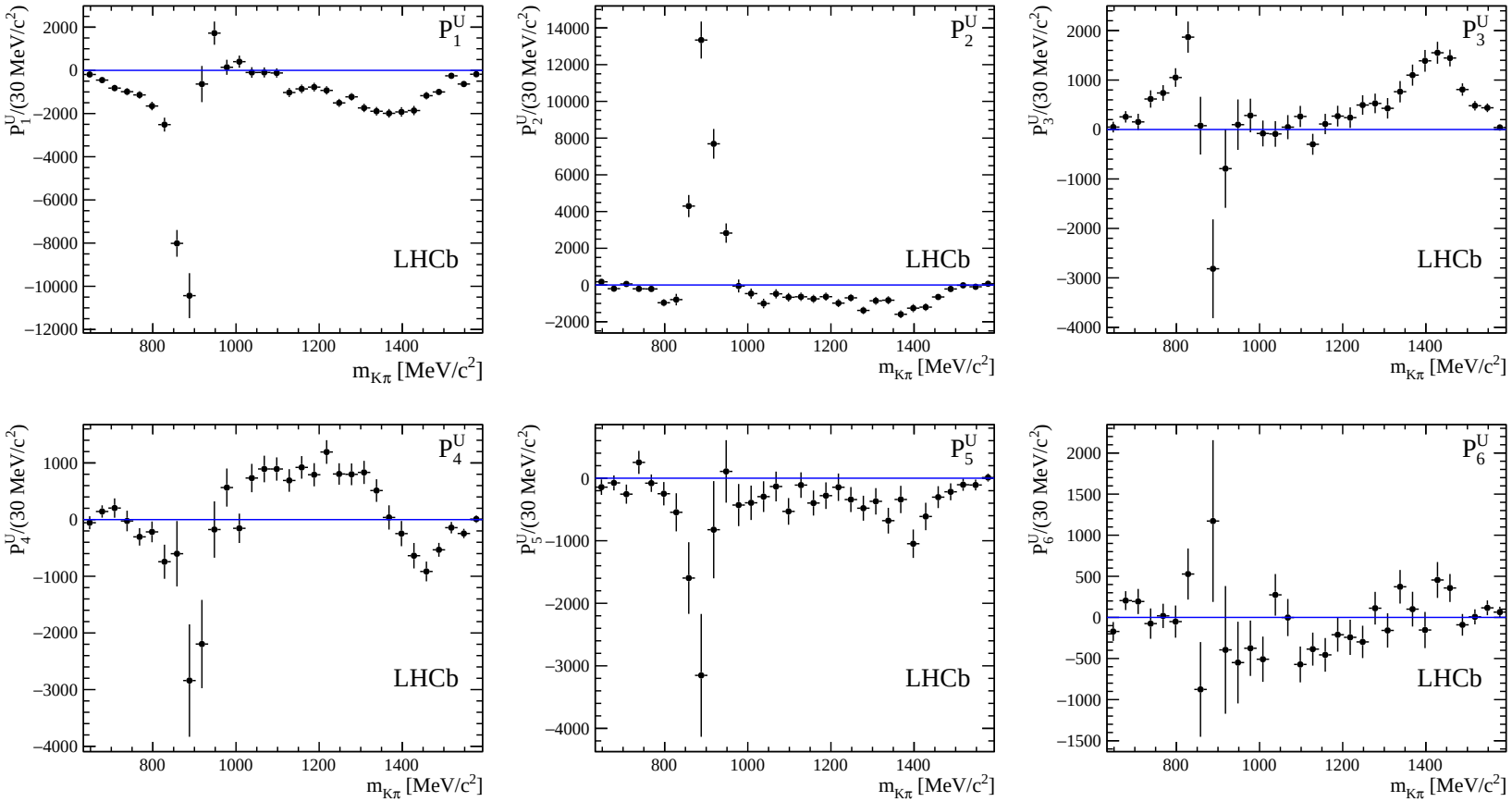

Model-independent confirmation of the exotic contribution.
Check that $K^-\pi^+$ amplitude fails to describe the amplitude.
$K^-\pi^+$ should contribute to reasonably low moments, while exotic $\psi'\pi^-$ contributes to *all* moments.

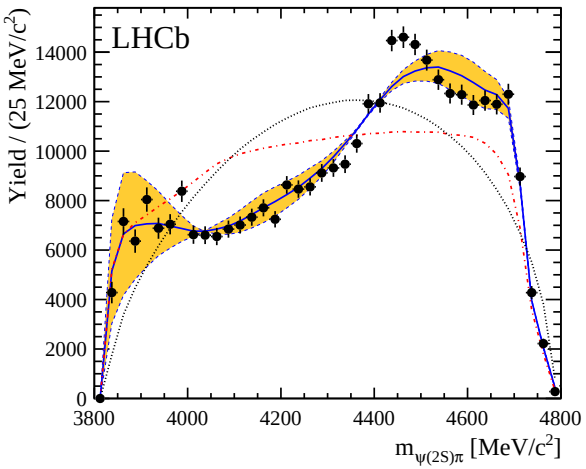

$l_{\max} = 4$

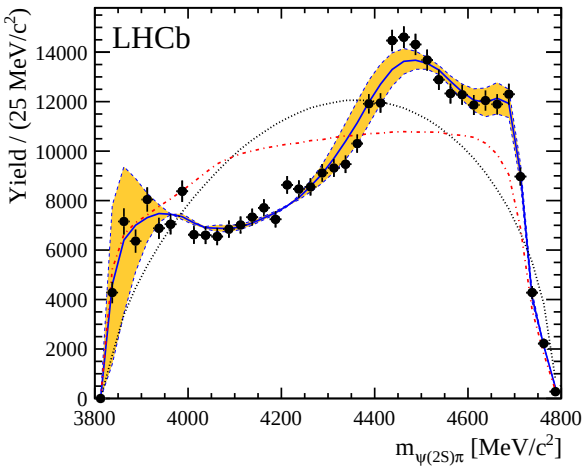

$l_{\max} = 6$

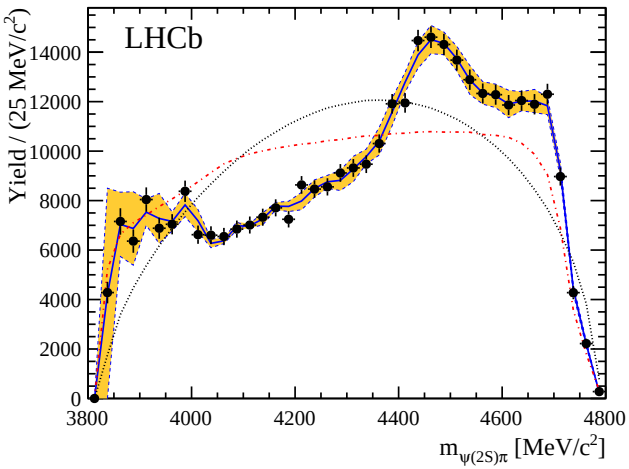

$l_{\max} = 30$

Test statistic:

$$-2\Delta NLL = -2 \sum_i \frac{W_i}{\epsilon_i} \log \frac{F_l(m^i_{\psi\pi})}{F_{30}(m^i_{\psi\pi})}$$

Run toys with $K^+\pi^-$-only model to determine distribution, compare with result in data.

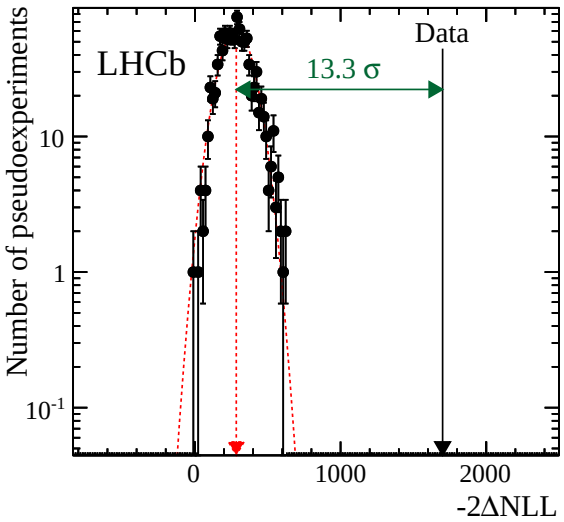

$l_{\max} = 4$

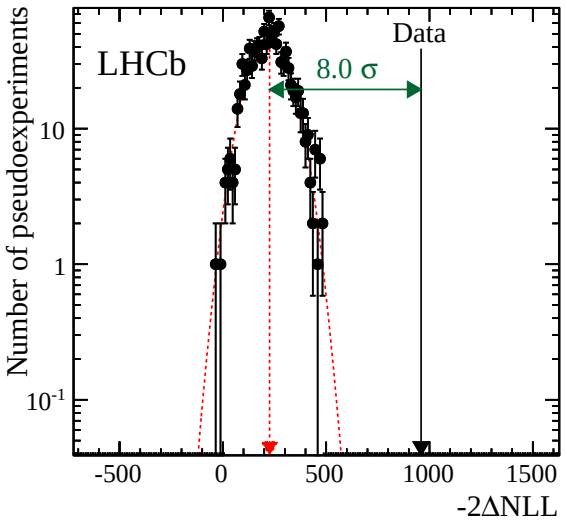

$l_{\max} = 6$

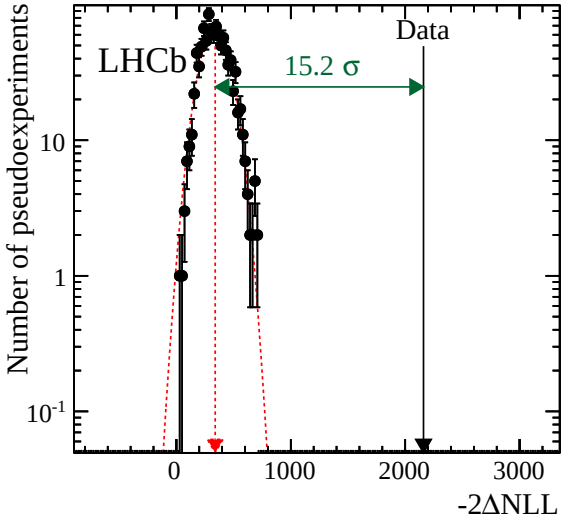

$l_{\max} = 4 \ldots 6$ depending on $m(K^+\pi^-)$

Non-scalars in the final state: $B^+ \to J/\psi\,\phi K^+$ [arXiv:1606.07898]

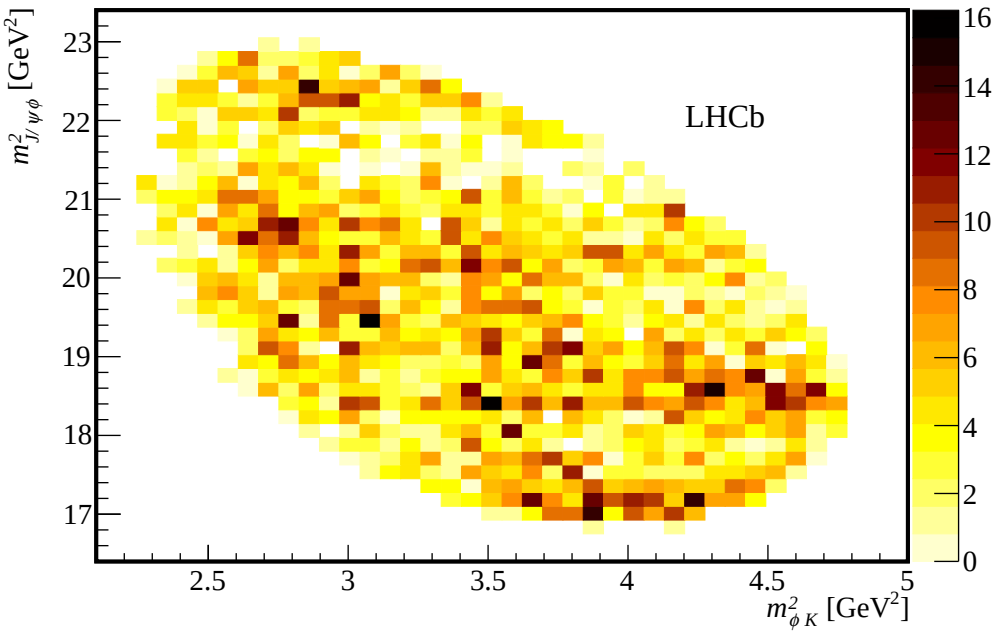

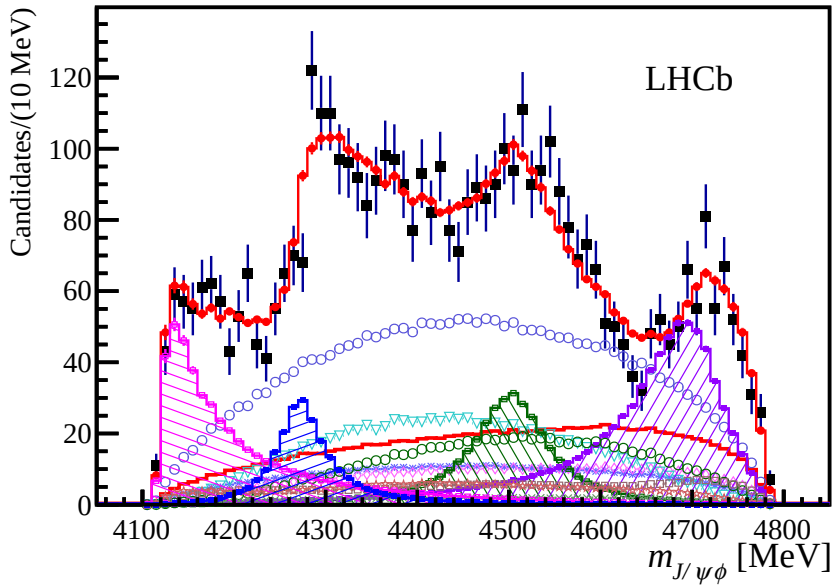

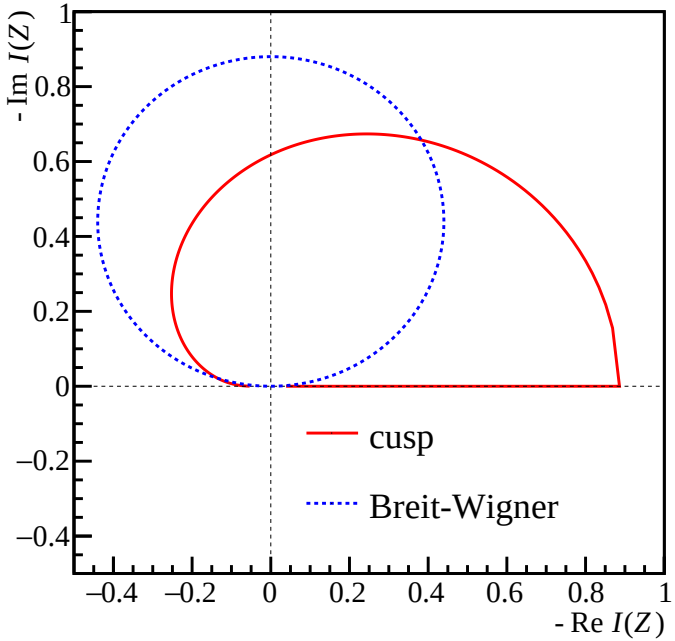

Statistics are not enough for model-independent lineashapes of X states.

More data should distinguish cusps and resonances

Non-scalars in the final state: $B^+ \to J/\psi\,\phi K^+$ [arXiv:1606.07898]

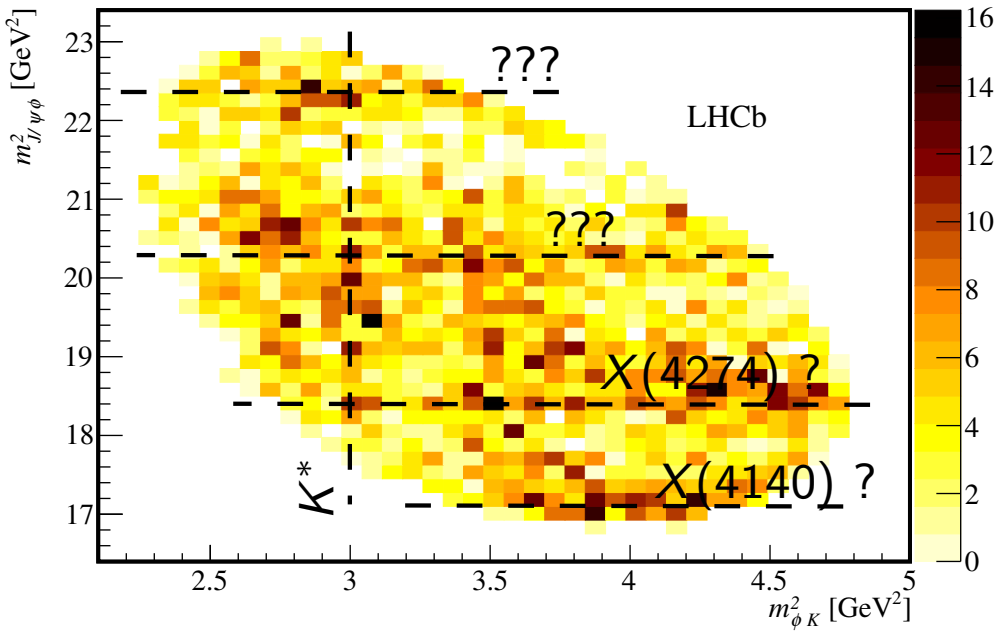

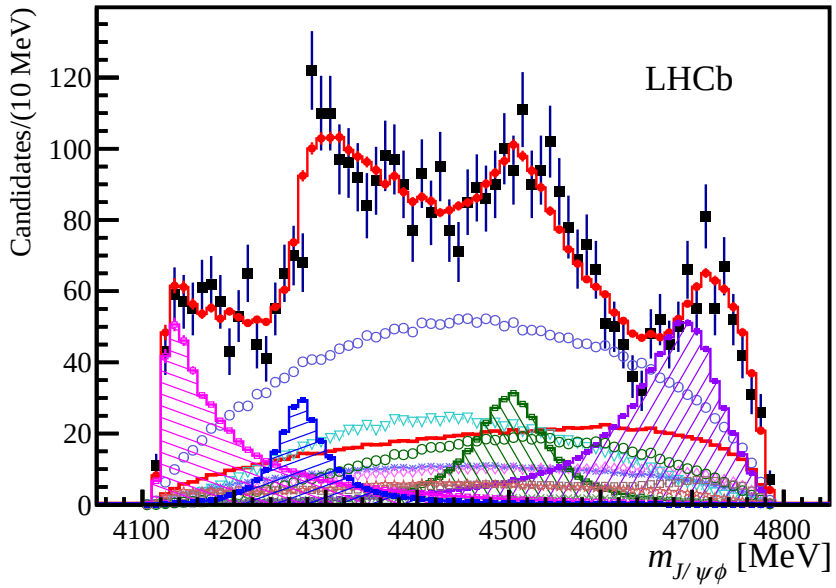

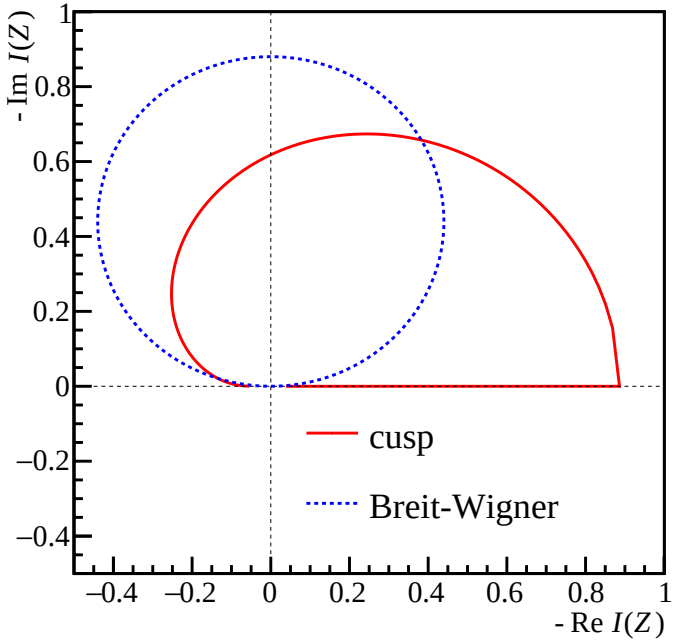

Statistics are not enough for model-independent lineashapes of X states.
More data should distinguish cusps and resonances

Initial state is not a pure quantum state.

- In general: polarisation (dependent on production kinematics).
- Longitudinal polarisation violates parity, transverse still possible.
- In case of Λ_b^0: polarisation consistent with zero at LHCb.

$\Lambda_b^0 \to J/\psi\, pK^-$: 6D phase space for polarised Λ_b^0 ($M_{K^-\pi^+}$ and 5 helicity angles)

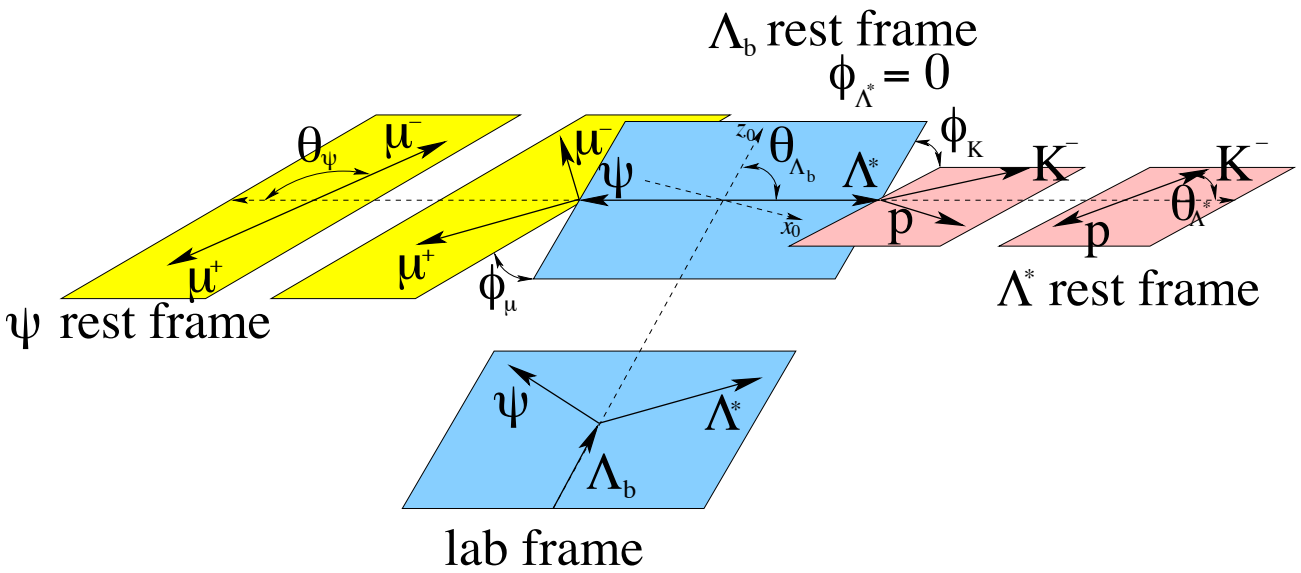

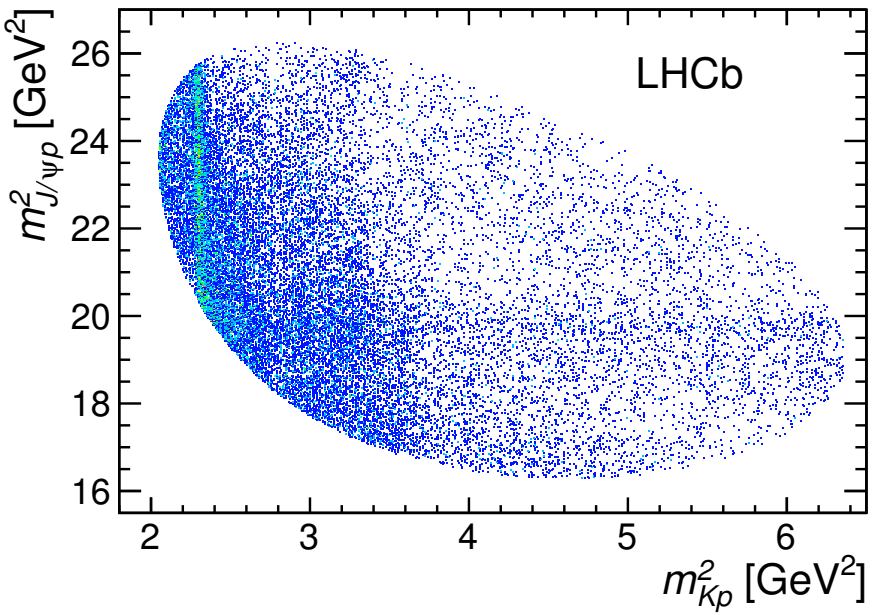

State	J^P	M_0 (MeV)	Γ_0 (MeV)	# Reduced	# Extended
$\Lambda(1405)$	$1/2^-$	$1405.1^{+1.3}_{-1.0}$	50.5 ± 2.0	3	4
$\Lambda(1520)$	$3/2^-$	1519.5 ± 1.0	15.6 ± 1.0	5	6
$\Lambda(1600)$	$1/2^+$	1600	150	3	4
$\Lambda(1670)$	$1/2^-$	1670	35	3	4
$\Lambda(1690)$	$3/2^-$	1690	60	5	6
$\Lambda(1800)$	$1/2^-$	1800	300	4	4
$\Lambda(1810)$	$1/2^+$	1810	150	3	4
$\Lambda(1820)$	$5/2^+$	1820	80	1	6
$\Lambda(1830)$	$5/2^-$	1830	95	1	6
$\Lambda(1890)$	$3/2^+$	1890	100	3	6
$\Lambda(2100)$	$7/2^-$	2100	200	1	6
$\Lambda(2110)$	$5/2^+$	2110	200	1	6
$\Lambda(2350)$	$9/2^+$	2350	150	0	6
$\Lambda(2585)$	?	$\approx$2585	200	0	6

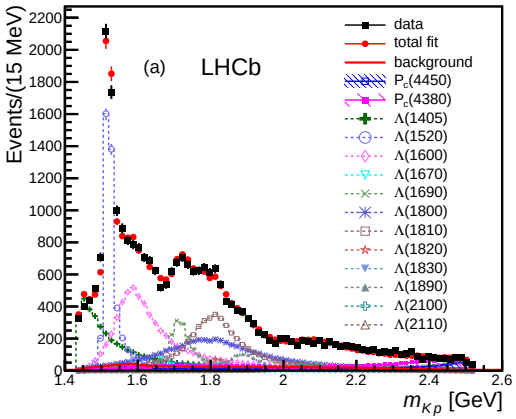

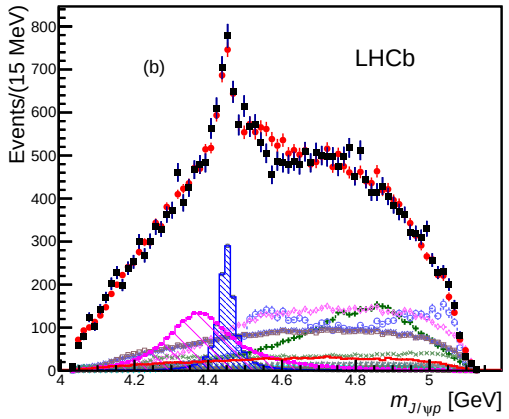

pK^- model: isobar with 12-14 Λ^* states from PDG.

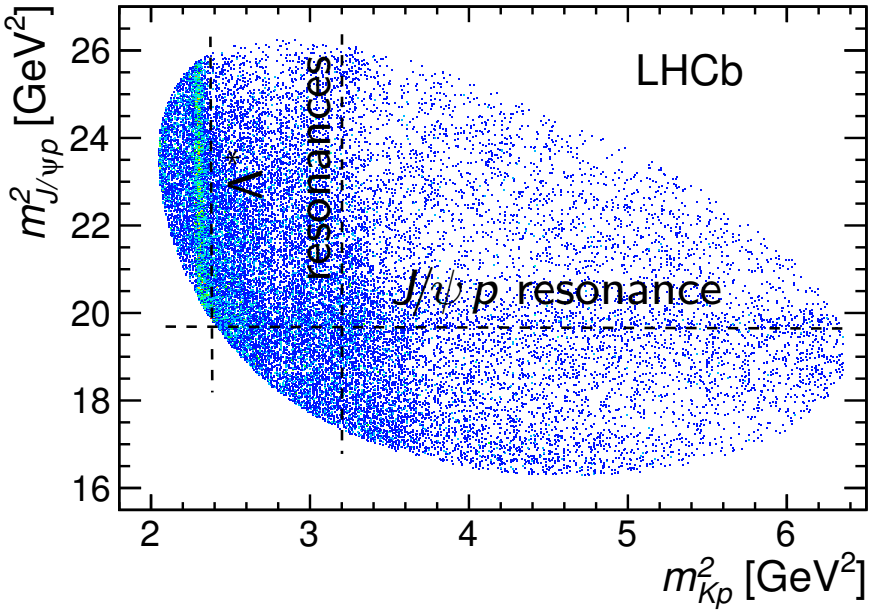

State	J^P	M_0 (MeV)	Γ_0 (MeV)	# Reduced	# Extended
$\Lambda(1405)$	$1/2^-$	$1405.1^{+1.3}_{-1.0}$	50.5 ± 2.0	3	4
$\Lambda(1520)$	$3/2^-$	1519.5 ± 1.0	15.6 ± 1.0	5	6
$\Lambda(1600)$	$1/2^+$	1600	150	3	4
$\Lambda(1670)$	$1/2^-$	1670	35	3	4
$\Lambda(1690)$	$3/2^-$	1690	60	5	6
$\Lambda(1800)$	$1/2^-$	1800	300	4	4
$\Lambda(1810)$	$1/2^+$	1810	150	3	4
$\Lambda(1820)$	$5/2^+$	1820	80	1	6
$\Lambda(1830)$	$5/2^-$	1830	95	1	6
$\Lambda(1890)$	$3/2^+$	1890	100	3	6
$\Lambda(2100)$	$7/2^-$	2100	200	1	6
$\Lambda(2110)$	$5/2^+$	2110	200	1	6
$\Lambda(2350)$	$9/2^+$	2350	150	0	6
$\Lambda(2585)$	?	$\approx$2585	200	0	6

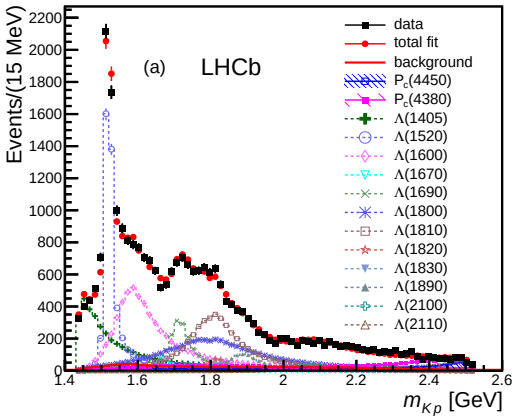

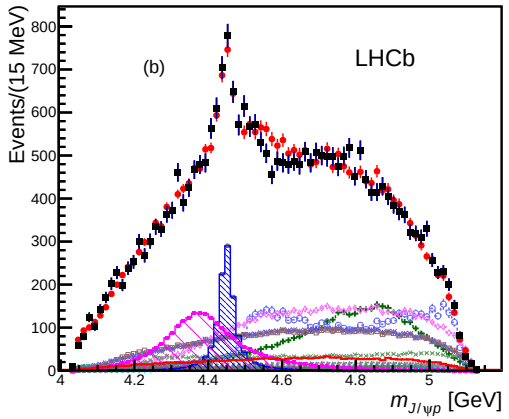

pK^- model: isobar with 12-14 Λ^* states from PDG.

Checking that K^* resonances only cannot describe the data.
Use Legendre moments in $\cos\theta_{\rm hel}$ as a function of m_{pK}.
Allow $l_{\rm max}$ depending on m_{pK}

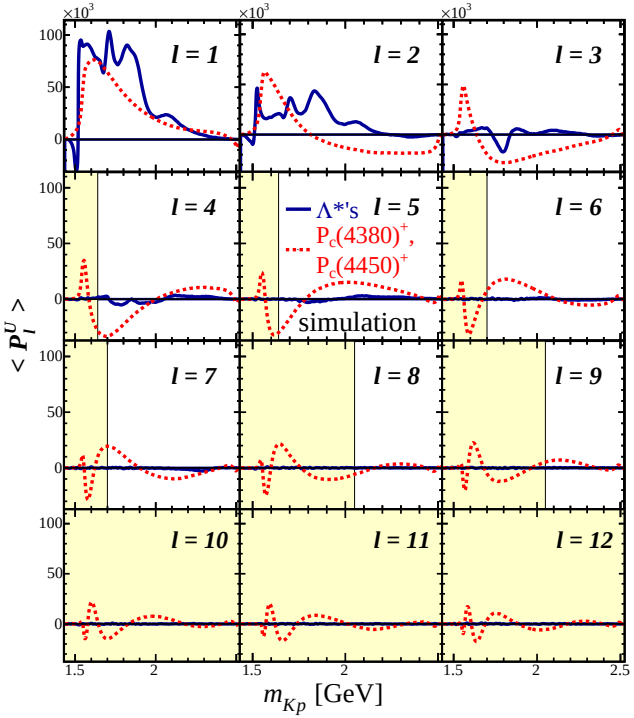

Moments from model

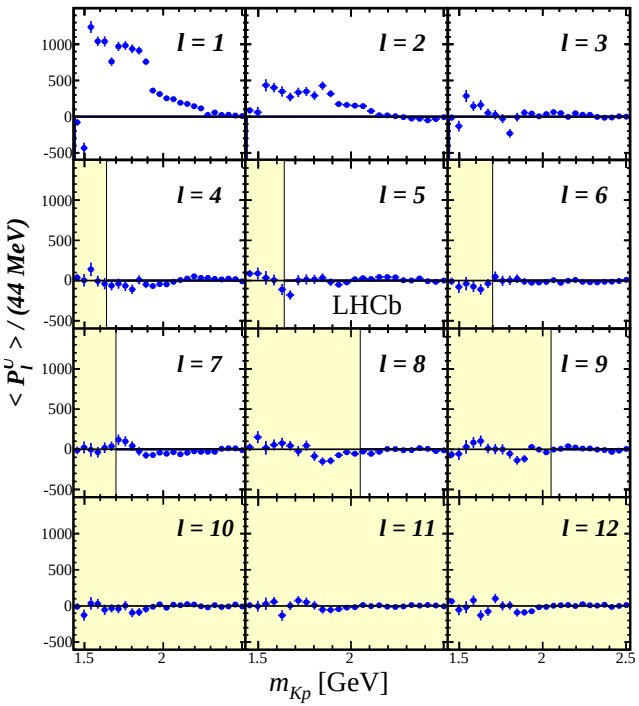

Moments from data

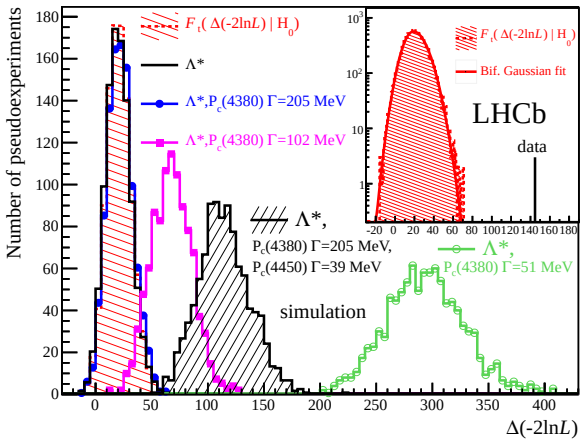

10σ significance

Conclusion

- Powerful analysis method
  - Not only spectroscopy: NP searches ($B \to K\pi\pi\gamma$), CP violation ($B \to$charmless)
- Challenges ahead:
  - Multibody decays $\Rightarrow$ multidimensional phase space
  - Sophisticated amplitude models beyond isobar
  - Very large datasets
- Efficient tools and human expertise are needed